

AD-776 005

POST-DOCTORAL RESEARCH IN SEISMOLOGY

Frank Press, et al

Massachusetts Institute of Technology

Prepared for:

Air Force Office of Scientific Research  
Advanced Research Projects Agency

31 August 1973

DISTRIBUTED BY:

**NTIS**

National Technical Information Service  
U. S. DEPARTMENT OF COMMERCE  
5285 Port Royal Road, Springfield Va. 22151

AD76005

Department of Earth and Planetary Sciences  
Massachusetts Institute of Technology  
Cambridge, Massachusetts 02139

POST-DOCTORAL RESEARCH IN SEISMOLOGY

Final Report to

Air Force Office of Scientific Research

1 July 1966 - 31 August 1973

ARPA Order No. - 1827-3

Program Code - 3F10

Name of Contractor - Massachusetts Institute of Technology

Effective Date of Contract - 1 July 1966

Contract Expiration Date - 31 August 1973

Amount of Contract - \$407,855.

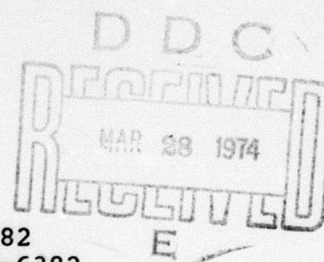
Contract No. - AF49(638)-1763

Principal Investigators - Frank Press, 617/253-3382  
M. Nafi Toksöz, 617/253-6382

Program Manager - William J. Best, 202/694-5456

Short Title of Work - Post-Doctoral Research in Seismology

Reproduced by  
NATIONAL TECHNICAL  
INFORMATION SERVICE  
U S Department of Commerce  
Springfield VA 22151



Sponsored by  
Advanced Research Projects Agency  
ARPA Order No. 1827-3

**AIR FORCE OFFICE OF SCIENTIFIC RESEARCH (AFSC)**  
**NOTICE OF TRANSMITTAL TO DDC**

This technical report has been reviewed and is  
approved for public release IAW AFR 190-12 (7b).  
Distribution is unlimited.

D. W. TAYLOR  
Technical Information Officer

ADDRESSER for	
WIS	White Section <input checked="" type="checkbox"/>
DDC	Ball Section <input type="checkbox"/>
WALL JENSEN	<input type="checkbox"/>
JUSTIFICATION	
BY	
DISSEMINATION/AVAILABILITY CODES	
WIS	ATL. and/or SPECIAL
A	

Qualified requestors may obtain additional copies from  
the Defense Documentation Center. All others should  
apply to the National Technical Information Service.

Approved for public release, distribution unlimited.

UNCLASSIFIED

-48-

AD 776005

Security Classification

## DOCUMENT CONTROL DATA - R &amp; D

(Security classification of title, body of abstract and indexing annotation must be entered when the overall report is classified)

1. ORIGINATING ACTIVITY (Corporate author) Massachusetts Institute of Technology Department of Earth & Planetary Sciences Cambridge, Massachusetts 02139		2a. REPORT SECURITY CLASSIFICATION UNCLASSIFIED	
3. REPORT TITLE  POST-DOCTORAL RESEARCH IN SEISMOLOGY		2b. GROUP	
4. DESCRIPTIVE NOTES (Type of report and inclusive dates) Scientific. ----- Final.			
5. AUTHOR(S) (First name, middle initial, last name) Frank Press M. Nafi Toksöz Jorge Mendiguren			
6. REPORT DATE 31 October 1973	7a. TOTAL NO. OF PAGES 52	7b. NO. OF REFS 56	
8a. CONTRACT OR GRANT NO. AF49(638)-1763	9a. ORIGINATOR'S REPORT NUMBER(S)		
b. PROJECT NO. AO 1827-3	9b. OTHER REPORT NO(S) (Any other numbers that may be assigned this report) AFOSR - TR - 74 - 0815		
c. 62701E	d.		
10. DISTRIBUTION STATEMENT Approved for public release, distribution unlimited.			
11. SUPPLEMENTARY NOTES  TECH, OTHER		12. SPONSORING MILITARY ACTIVITY AFOSR (NPG) 1400 Wilson Blvd. Arlington, Virginia 22209	
13. ABSTRACT  This is the final annual report for the contract entitled "Post-Doctoral Research in Seismology" which was initiated on July 1, 1966 and was carried out by many research associates with the collaboration of the staff members of the Department of Earth and Planetary Sciences and Lincoln Laboratory. This report describes the work of Jorge Mendiguren who was supported by the contract during the period of September 1972 to August 1973. A summary listing of publications for the entire period of July 1, 1966 to August 31, 1973 is also given.			

Reproduced by  
NATIONAL TECHNICAL  
INFORMATION SERVICE  
U S Department of Commerce  
Springfield VA 22151

DD FORM 1 NOV 65 1473

UNCLASSIFIED

Security Classification

UNCLASSIFIED

1d  
Department of Earth and Planetary Sciences  
Massachusetts Institute of Technology  
Cambridge, Massachusetts 02139

POST-DOCTORAL RESEARCH IN SEISMOLOGY

Final Report to  
Air Force Office of Scientific Research  
1 July 1966 - 31 August 1973

ARPA Order No. - 1827-3

Program Code - 3F10

Name of Contractor - Massachusetts Institute of Technology

Effective Date of Contract - 1 July 1966

Contract Expiration Date - 31 August 1973

Amount of Contract - \$407,855.

Contract No. - AF49(638)-1763

Principal Investigators - Frank Press, 617/253-3382  
M. Nafi Toksöz, 617/253-6382

Program Manager - William J. Best, 202/694-5456

Short Title of Work - Post-Doctoral Research in Seismology

Sponsored by  
Advanced Research Projects Agency  
ARPA Order No. 1827-3

ABSTRACT

This is the final annual report for the contract entitled "Post-Doctoral Research in Seismology" which was initiated on July 1, 1966 and was carried out by many research associates with the collaboration of the staff members of the Department of Earth and Planetary Sciences and Lincoln Laboratory. This report describes the work of Jorge Mendiguren who was supported by the contract during the period of September 1972 to August 1973. A summary listing of publications for the entire period of July 1, 1966 to August 31, 1973 is also given.

TABLE OF CONTENTS

ABSTRACT	Page i
Identification of Free Oscillation Spectral Peaks Using the Excitation Criterion	1
Summary of Publications for the Entire Contract Period	44

Identification of Free Oscillation Spectral  
Peaks Using the Excitation Criterion

In this final annual report, we describe the work of Jorge Mendiguren on the identification of free oscillation spectral peaks by the new powerful method called "excitation criterion". An intensive search of higher modes was done using data for the July 30, 1970 Colombian deep shock. Spheroidal oscillations, ranging from the fundamental to the sixth higher overtone, and torsional oscillations up to the third higher overtone were identified. Spheroidal oscillations for periods smaller than 100 seconds were clearly identified for the third and fifth overtone.

The standard deviation of the measurements was estimated applying the excitation criterion to different subsets of stations. Some of the eigenperiods measured for higher overtones, especially the third and fifth overtones at periods near 100 seconds were found to be very stable. Discrepancies between eigenperiods for different subsets of stations are as small as 0.01%. This is in agreement with the idea of a lower mantle with less important lateral heterogeneities than the upper mantle.

Comparison of the eigenperiods determined for both the Alaskan 1964 and the Colombian 1970 earthquakes showed

systematic differences. That difference is of the order of 0.3% for  ${}_0T$  modes while for  ${}_0S$  modes it is much smaller, around 0.04%. There are indications that such a discrepancy is also present for overtones. This means that the lateral heterogeneities of the earth are such that, even with good coverage of stations, the average eigenperiods measured for shocks with different epicenters and source mechanisms will be different by a measurable amount.

The effect of the source finiteness on the spectral resolution was theoretically analyzed. We found that for oscillations with wavelengths about 6 times the source linear dimension or longer, the effect of source dimension is not too important. A simple point source can be assumed if we discard those stations where the theoretical amplitude of the mode under study is ~2.5 times smaller than the average amplitude computed for all the stations.

The following paper by Mendiguren is reprinted from the Geophysical Journal of the Royal Astronomical Society, 33, 1973.

## Identification of Free Oscillation Spectral Peaks for 1970 July 31, Colombian Deep Shock using the Excitation Criterion

Jorge A. Mendiguren

(Received 1973 February 26)\*

### Summary

The excitation criterion was applied to identify spectral peaks of free oscillations excited by the Colombian deep shock of 1970 July 31. About 160 new overtones were identified. They range from  ${}_1T$  to  ${}_3T$  torsional modes and from  ${}_1S$  to  ${}_6S$  spheroidal modes. Some of the modes identified have periods below 90 s. The standard deviation of the measured eigenperiods is in general smaller than 0.1%. Comparison of  ${}_6S$  and  ${}_0T$  eigenperiods measured for the Alaskan (1964) and Colombian shocks shows a systematic difference. The difference is larger than the error of the measurement, and this indicates that the average eigenfrequencies measured for each event are biased by the epicentre location. The effect of lateral heterogeneities of the Earth, aftershocks, and the choice of source and Earth model when using the excitation criterion are discussed in detail.

### 1. Introduction

In recent years there has been an increasing emphasis on the use of free oscillation data to derive models of the Earth's interior, e.g. Press (1968), Haddon and Bullen (1969), Dziewonski & Gilbert (1972a), Johnson (1972). Most of the free oscillation data available for those studies correspond to modes with periods longer than 250-300 s. But it is clear that additional higher mode data will be necessary for a more detailed determination of the Earth structure (Wiggins 1972), and therefore new identifications of overtones at shorter periods are highly desirable.

Unfortunately, for periods below 250-300 s it is not possible to obtain unambiguous results using the conventional methods of spectral peak identification (Dziewonski & Gilbert 1972a). Those methods consist of comparing theoretical to observed eigenfrequencies, combined with some additional criterion based on the difference in polarization for different modes (e.g. Benioff, Press & Smith 1961; Ness, Harrison & Slichter 1961), or separation of shear and volumetric strains (e.g. Nowroozi 1965; Smith 1966). Some of the limitations of these methods can be avoided using the differential attenuation criterion proposed by Dratler *et al.* (1971), and extensively used by Dziewonski & Gilbert (1972b) for periods below 250 s. This method is based on the difference in attenuation for different modes, and can be applied to identify spheroidal modes with high  $Q$  values.

Another method which can be used at short periods is the criterion based on the ray-mode duality; originally proposed by Brune (1964), it was later used by Alsop &

\*Received in original form 1973 February 9.

Brune (1965) and Nowroozi (1972). The identifications obtained using this method have not been critically tested yet, and additional applications are necessary for a clear evaluation of its practical merits.

Unlike the earlier methods, the excitation criterion (Mendiguren 1972a, b, c, 1973) renders reliable identifications at all periods and can be applied to torsional as well as spheroidal modes, even in those cases with low  $Q$  values. Theoretically this method should work for any well-excited mode if its amplitude and phase at the observing stations can be predicted using a suitable Earth and source model.

In the following sections, the excitation criterion is discussed in more detail than in former publications. And finally the results of its application to the free oscillations excited by the Colombian deep shock of 1970 July 31 are thoroughly displayed.

## 2. Theoretical and observed spectra of free oscillations

The basic assumption underlying the excitation criterion is that the observed spectra of free oscillations can be predicted using suitable models for the Earth and the source mechanism.

In this section it will be shown that for the case of the free oscillations excited by the Colombian deep shock of 1970 July 31, a simple double-couple source in a laterally homogeneous earth is an adequate model to predict the spectra of the fundamental spheroidal modes. In later sections this simple model is successfully used in the excitation criterion scheme to identify higher modes uniquely, and this indirectly proves that this model is also suitable to predict the spectra of overtones. Saito's formulae (Saito 1967) have been used in this study to compute the theoretical spectra.

The displacement spectra of free oscillations excited by a double-couple source, having a step function as source time function and being imbedded in a laterally homogeneous earth can be expressed as follows (Saito 1967):

$$U^T = \sum_n \sum_{m=0}^2 \sum_j \frac{A_{n,m,j}}{\omega_{n,j}^2} Y_1^T(a) T_n^m(\theta, \phi) e^{i\omega_{n,j} t} \quad (1)$$

$$U^S = \sum_n \sum_{m=0}^2 \sum_j \frac{B_{n,m,j}}{\omega_{n,j}^2} \{ Y_1^S(a) S_1^{m,n}(\theta, \phi) + Y_3^S(a) S_2^{m,n}(\theta, \phi) \} e^{i\omega_{n,j} t} \quad (2)$$

where

$r, \theta, \phi$  = spherical co-ordinate system;  $r$  is measured from the centre of the Earth; the  $\theta = 0$  axes passes through the hypocentre;  $\phi$  is measured counterclockwise from the fault strike direction.

$j$  = radial order number.

$n$  = co-latitudinal order number; order of Legendre polynomial.

$m$  = azimuthal order number; degree of Legendre polynomial.

$a$  = Earth radius.

$\omega_{n,j}$  = angular eigenfrequency corresponding to the mode of radial order  $j$ .

$t$  = time measured from the source origin time.

$S, T$  = superscripts indicating spheroidal and torsional modes.

$Y_1^S, Y_3^S$  = radial and  $\theta$  displacement eigenfunctions for spheroidal modes.

$Y_1^T$  =  $\phi$  displacement eigenfunction for torsional modes.

$A, B$  = coefficients which are functions of focal depth, Earth model and orientation of the double couple.

$T_n^m(\theta, \phi), S_1^{m,n}(\theta, \phi), S_2^{m,n}(\theta, \phi)$  = vector spherical harmonics

Identification of free oscillation spectral peaks

283

	$r$	$\theta$	$\phi$	
$T_n^m(\theta, \phi)$	0	$\frac{1}{\sin \theta} \frac{\partial Y_n^m}{\partial \phi}$	$\frac{-\partial Y_n^m}{\partial \theta}$	
$S_{1,n}^m(\theta, \phi)$	$Y_n^m$	0	0	(3)
$S_{2,n}^m(\theta, \phi)$	0	$\frac{\partial Y_n^m}{\partial \theta}$	$\frac{1}{\sin \theta} \frac{\partial Y_n^m}{\partial \phi}$	

where

$$Y_n^m(\theta, \phi) = P_n^m(\cos \theta) \begin{pmatrix} \cos \\ \sin \end{pmatrix} m \phi$$

The hypocentre parameters used to compute 1 and 2 are those given by NOAA:

Origin time            17 h 08 m 5.4 s  
 Latitude                1.5° S  
 Longitude              72.6° W  
 Depth                  651 km  
 (Magnitude  $m_b = 7.1$ )

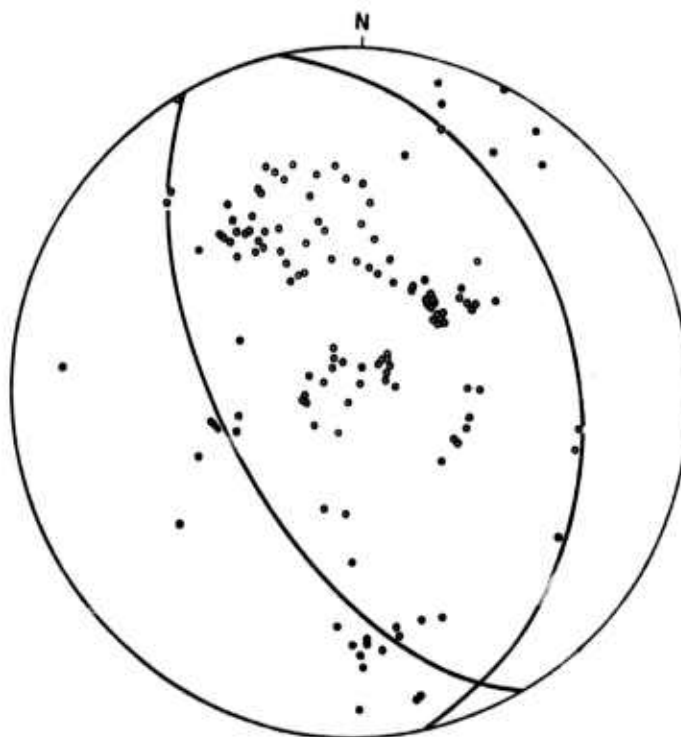


FIG. 1. Equal area projection of the lower hemisphere. Open and full circles indicate dilatations and compressions, respectively.

The nodal plane solution needed to compute A and B was derived from *P* wave observations (Mendiguren 1972a) and it is shown in Fig. 1. Its parameters are:

	Dip direction	Dip	Trend	Plunge
Plane a	N 122° W	58°		
Plane b	N 75° E	32°		
Pressure axis			N 32° E	75°
Tension axis			N 116° W	12°
Null axis			N 153° E	8°

The HBI-6 Earth model of Haddon & Bullen (1969) was adopted in this study but, as discussed in Section 6, the selection of the Earth model is not critical in the excitation criterion scheme. The corresponding free oscillations eigenfunctions were computed using a program written by R. Wiggins (1968). Theoretical spectra were computed for 83 WWSSN stations, while the observed spectra was obtained from long period seismometer records at those stations. A list of the stations is given in the Appendix. The method of data processing is also described in the Appendix.

Figs 2 and 3 show the resulting theoretical radial displacement spectra for fundamental spheroidal modes compared to the observed ones at 20 stations. The main features of the observed spectra are closely reproduced by the theoretical spectra of

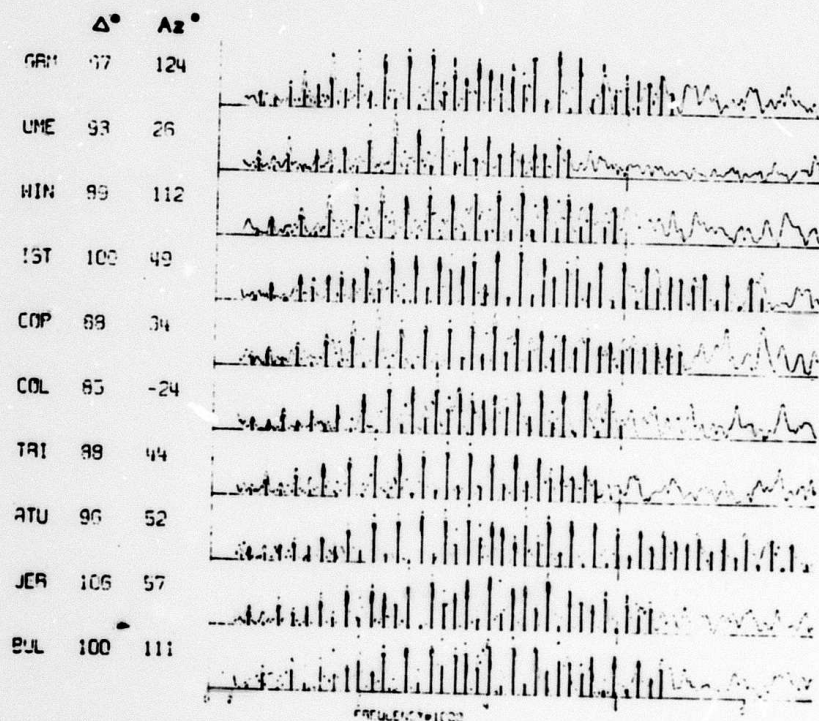


FIG. 2. Continuous lines indicate the observed radial displacement spectrum. Vertical bars are the theoretical spectral lines.  $\Delta$  is the epicentral distance.  $Az$  is the azimuth at the epicentre measured clockwise from north. The pattern of alternating large and small amplitude peaks is characteristic of stations near  $\Delta = 90^\circ$ .

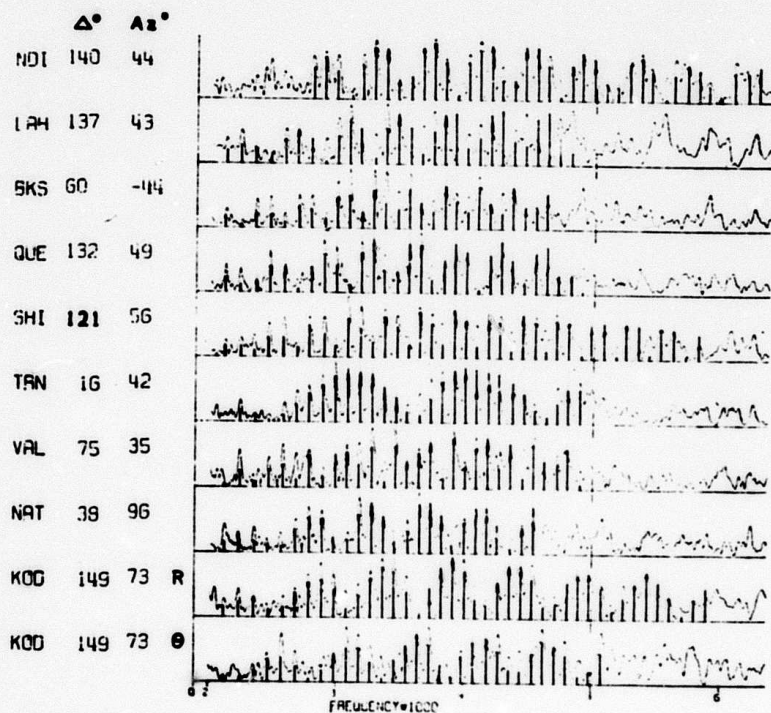


FIG. 3. Continuous lines indicate the observed radial displacement spectrum. Vertical bars are the theoretical spectral lines.  $\Delta$  is the epicentral distance.  $Az$  is the azimuth of the epicentre measured clockwise from north. Note the shift in nodes between the  $\theta$  and R spectra for KOD.

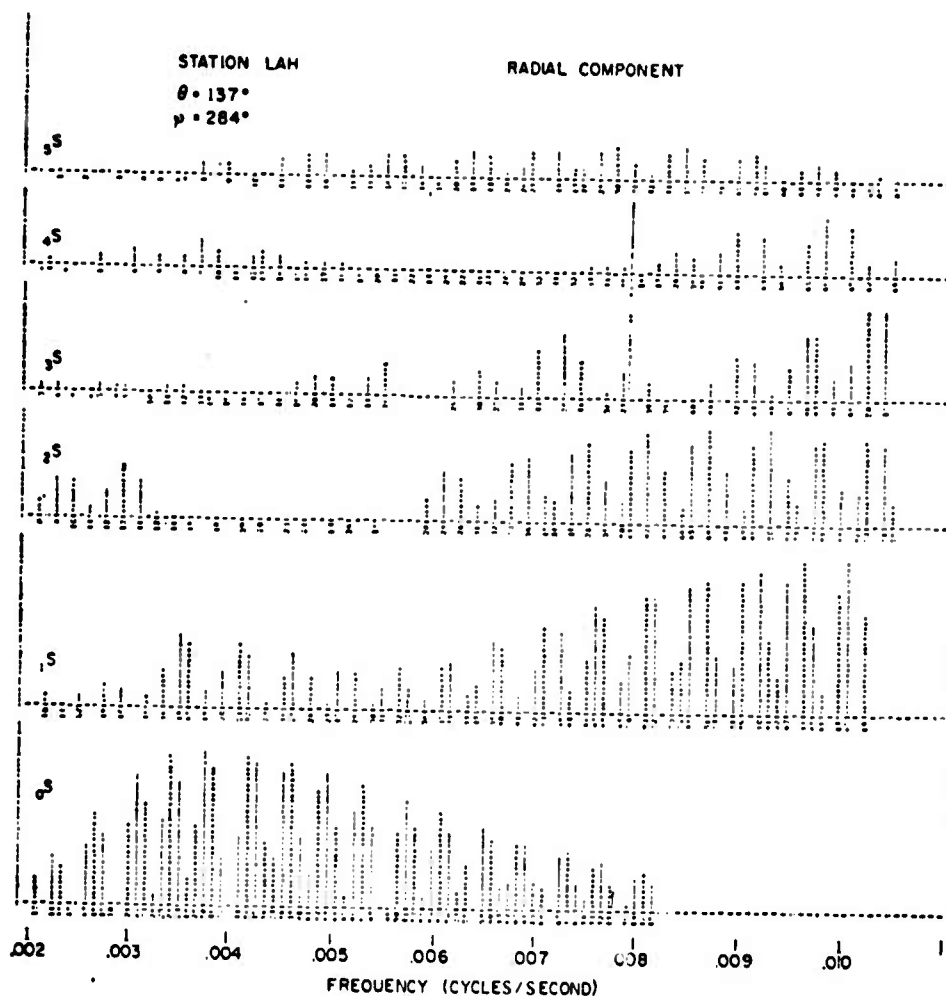


FIG. 4. Theoretical line spectra of the radial displacement of spheroidal oscillations at LAH. Numbers under each line indicate the co-latitudinal order number. '+' and '1' indicate that the phase of the mode is 0 or  $\pi$  respectively.

$0S$  modes. The  $0S$  spectra explain by itself most of the observed spectral features because as shown in Fig. 4 for LAH station,  $0S$  dominates the vertical displacement at that frequency range. The amplitude of the other modes is much smaller. The same occurs at all other stations.

The close agreement shown in Figs 2 and 3 indicates that a point source in a laterally homogeneous Earth is an adequate model to predict the actual displacement spectra for this event. Limitations of this simple model due to lateral heterogeneities of the real Earth and source finiteness will be discussed in later sections.

### 3. The excitation criterion applied to the spectra observed at a single station

The close agreement shown in Figs 2 and 3 suggests that a simple method to identify spectral peaks is to compare theoretical to observed spectra at single stations. This technique was applied to the oscillations excited by the Colombian shock and many overtones were identified. Some examples of those identifications on spectra obtained from records of WWSSN stations and the NE strainmeter at Nana (Puru) are shown in this section.

Identification of free oscillation spectral peaks

287

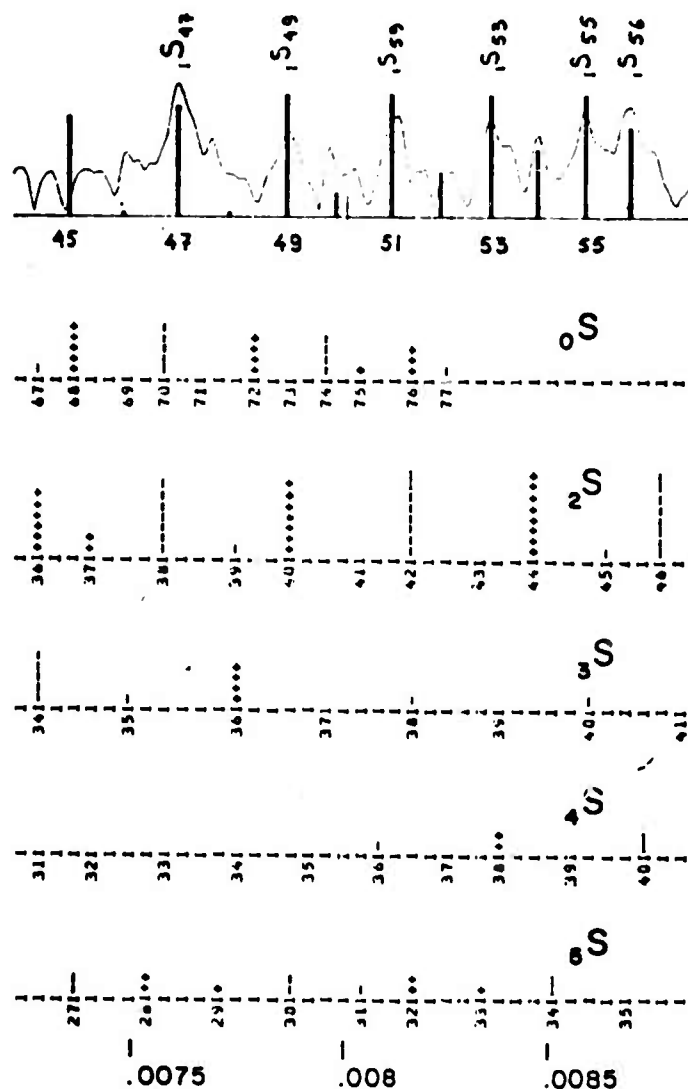


FIG. 5. Theoretical and observed spectra of the radial displacement component at KEV. The numbers under the theoretical line spectra indicate the co-latitudinal order number. '+' and 'I' indicate that the phase of the mode is 0 or  $\pi$  respectively.

Fig. 5 shows part of the radial component spectrum observed at KEV compared to the theoretical spectra of different spheroidal modes. The identifications of the  $1S$  peaks are based on the dominant excitation expected for those modes and the agreement between the theoretical shape of the  $1S$  spectrum and the main features of the observed one. The other modes are not so well excited and the spacing between theoretical peaks does not match the observed one.

In a similar way, Fig. 6 shows  $2S$  peaks identified in the co-latitudinal displacement spectra at ESK.  $3S$  modes identified at ATU are shown in Fig. 7.

Usually the  $3S$  peaks in the colatitudinal component spectra are confusingly mixed with  $0S$  peaks in the frequency range shown in Fig. 8, but in the particular case of BOG the extended node in the  $0S$  spectra makes the  $3S$  peaks clearly visible. The theoretical prediction of the node in  $0S$  spectra gives support to those identifications. At both sides of the node the identifications are less reliable.

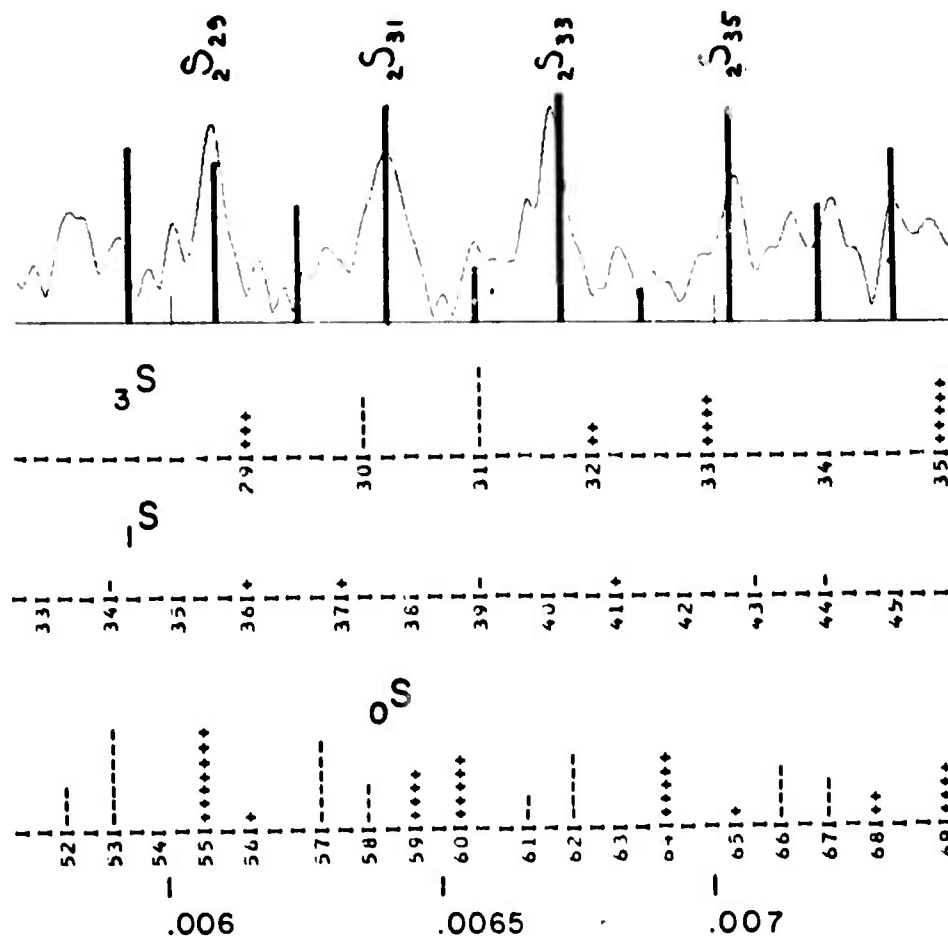


FIG. 6. Theoretical and observed spectra of the co-latitudinal displacement component at ESK.

The spheroidal modes have an azimuthal displacement component of very small amplitude when compared to the radial or co-latitudinal ones and their corresponding peaks have never been observed before. As their amplitude goes like  $1/\sin \theta$  (see the  $\phi$  component of  $S_{2,n}^m$  in expression (3)) they only could be observed close to the epicentre or its antipodes. Fig. 9 shows some of those peaks corresponding to the  ${}_0S$  modes identified in an extended node of the  ${}_0T$  spectra at BOG, only 60.0 km from the epicentre. At both sides of the node of  ${}_0T$  the peaks are confusedly intermixed and no clear identification is possible. Fig. 10 shows a more complete theoretical spectra of the azimuthal component at BOG. Only the knowledge of the theoretical spectra makes those identifications reliable.

The strain spectra observed by the NE component strainmeter at NNA is shown in Fig. 11 in comparison with the theoretical one. As the NE component strainmeter is directed at an angle  $\alpha = 17^\circ$  from the station to epicentre direction, its spectrum shows intermixed torsional and spheroidal peaks. The theoretical strain was computed as a function of the  $c_{\theta\theta}$ ,  $c_{\phi\phi}$ ,  $c_{\phi\theta}$  strains as follows.

$$e_{\alpha\alpha} = c_{\theta\theta} \cos^2 \alpha + c_{\phi\phi} \sin^2 \alpha + c_{\phi\theta} \sin \alpha \cos \alpha$$

$e_{\theta\theta}$ ,  $e_{\phi\phi}$  and  $c_{\phi\theta}$  were computed taking appropriate derivatives of the displacement given by expressions (1) and (2). The agreement shown in Fig. 11 indicates that our simplified source and Earth models are also valid at the lowest frequency range.

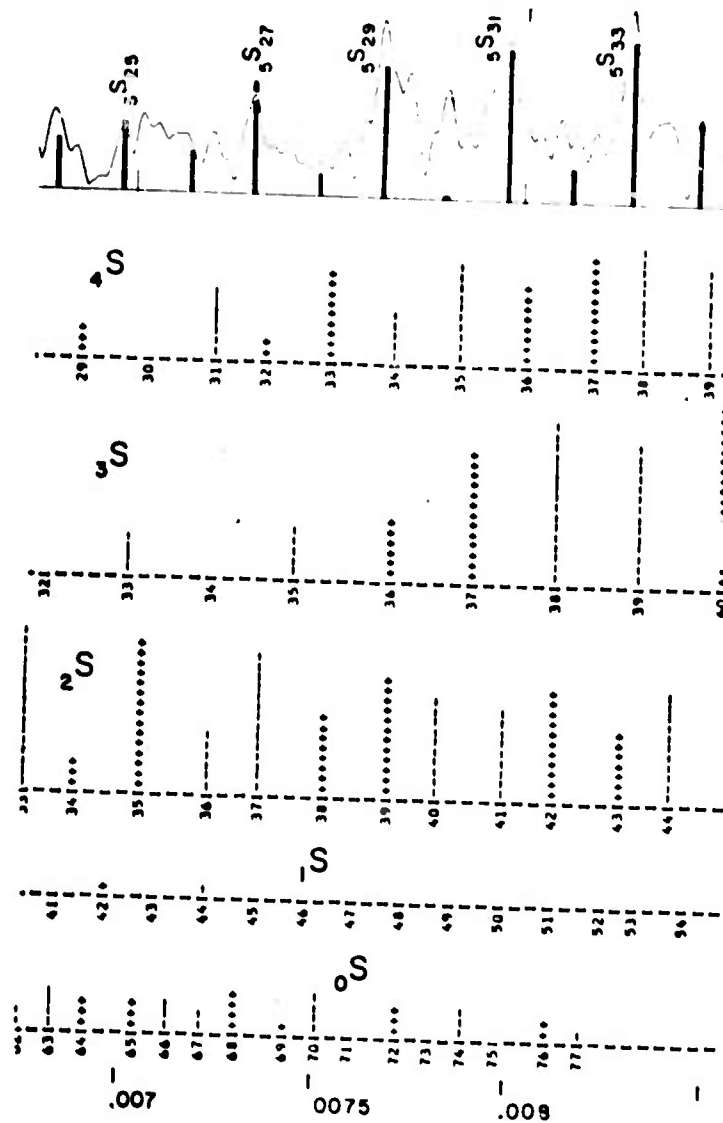


FIG. 7. Theoretical and observed spectra of the co-latitudinal displacement component at ATU.

J. A. Mendiguren

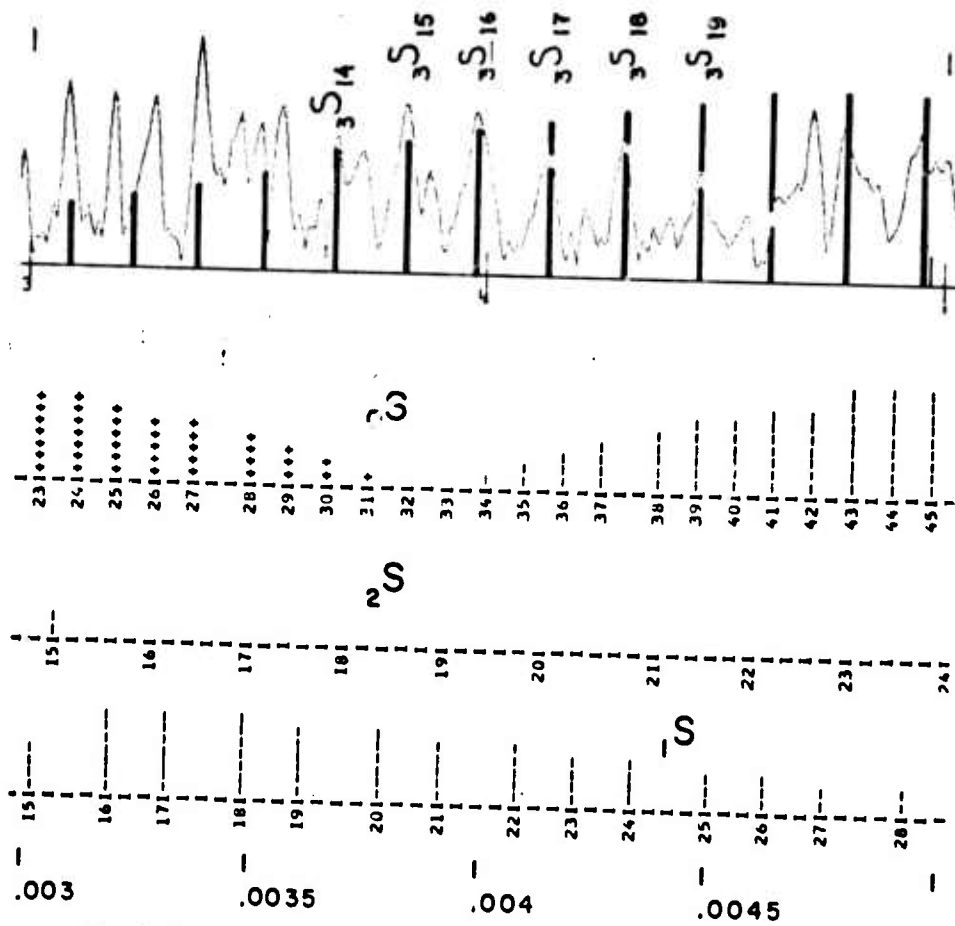


FIG. 8. Theoretical and observed spectra of the co-latitudinal displacement component at BOG.

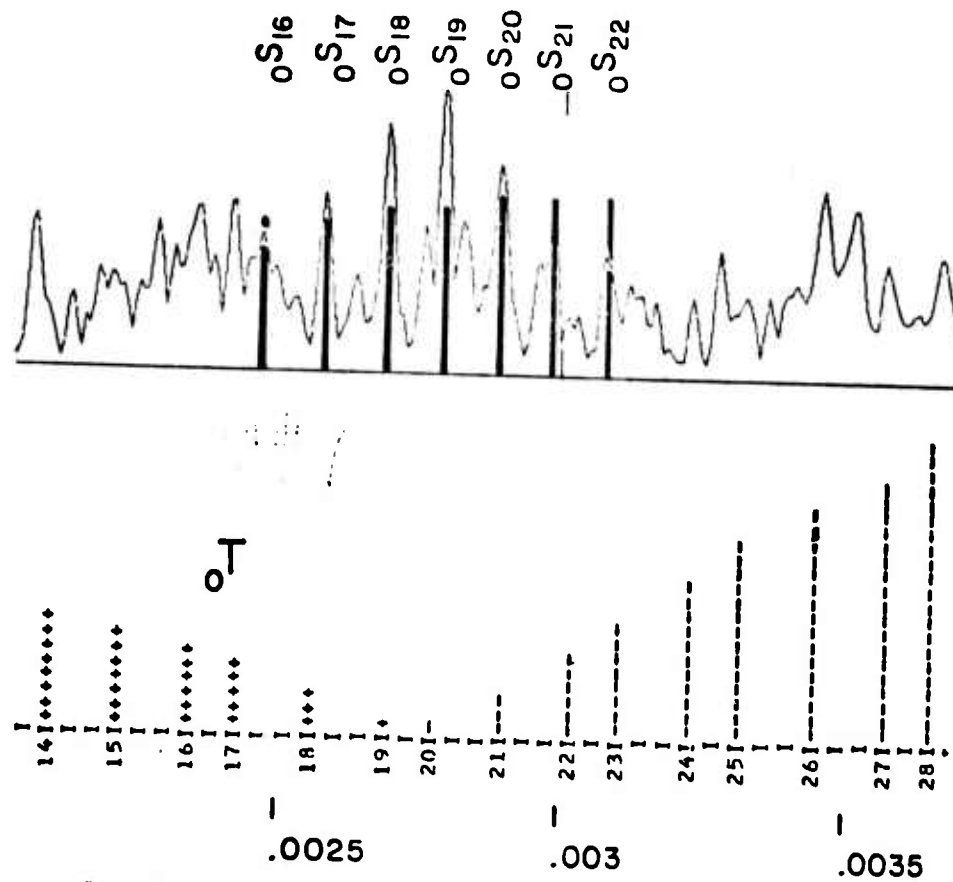


FIG. 9. Theoretical and observed spectra of the azimuthal displacement component at BOG.

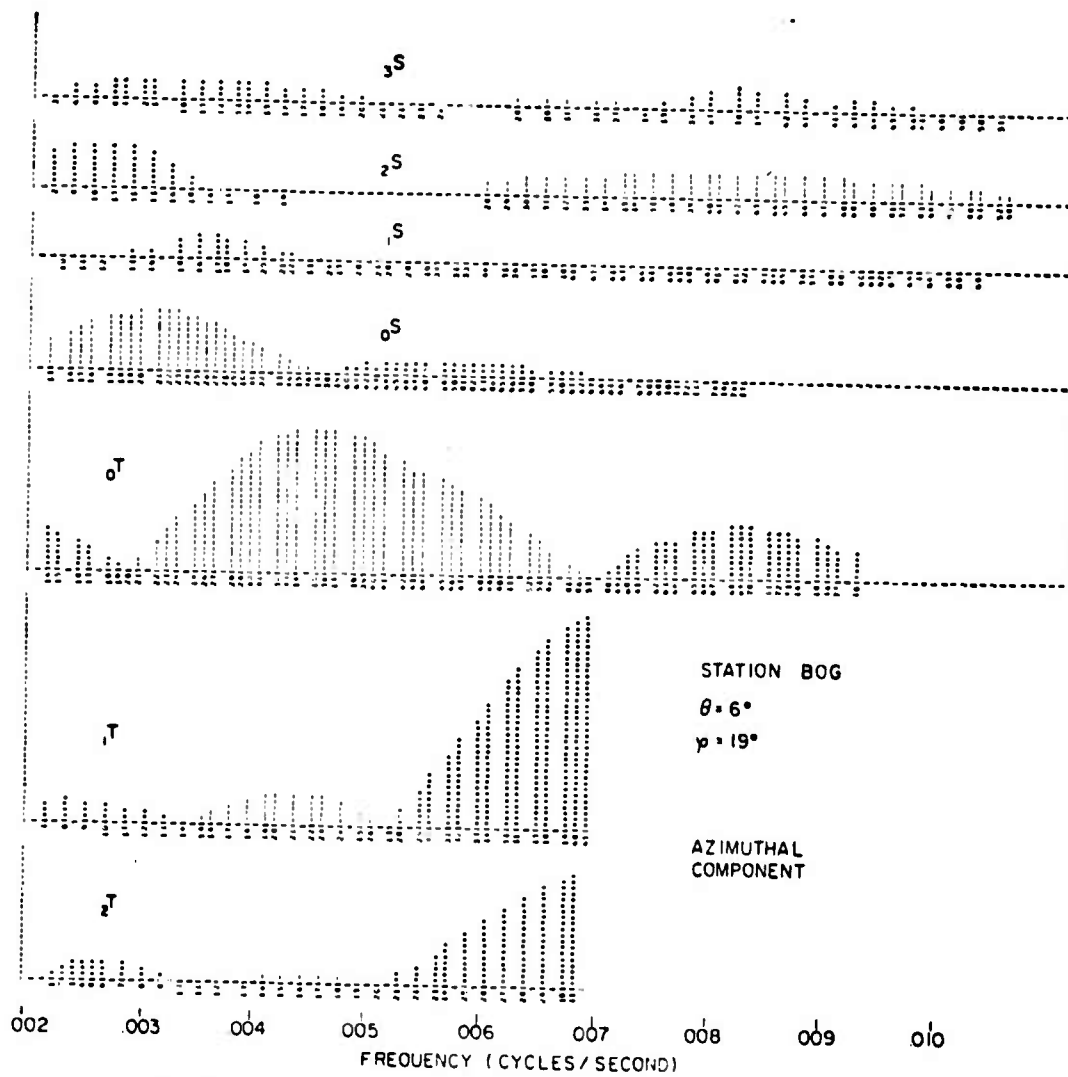


FIG. 10. Theoretical spectra of the azimuthal displacement component at BOG.

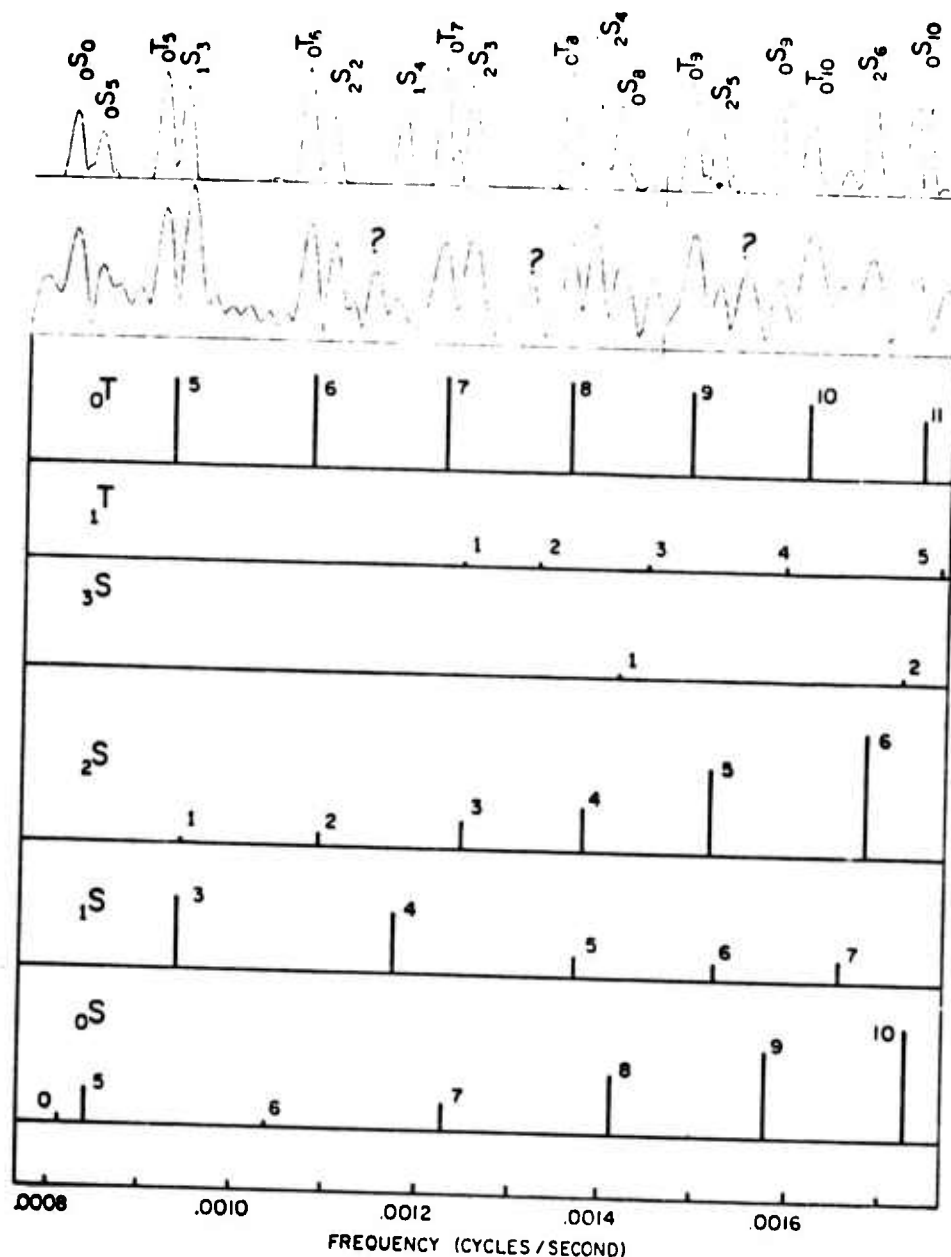


FIG. 11. Observed and theoretical strain spectrum for the N39° E strainmeter at NNA. The observed spectrum is the second from the top. The spectrum at the top results from the convolution of the theoretical line spectrum with a  $\sin x/x$  function simulating the effect of the finite record length.  $0T$  modes have been slightly displaced toward lower frequencies to match the observations.  $0S_0$  and  $1S_3$  to  $1S_4$  require larger amplitudes to match the observations. Those observed peaks indicated with a question mark have not a theoretical equivalent and are attributed to recording noise.

All these examples indicate that if the spectra at only a few stations are available, some of the observed peaks can be identified by comparing theoretical to observed amplitude spectra at single stations. Usually this approach renders more convincing identifications when only one mode dominates the spectrum, like the  ${}_2S$  modes in Fig. 6. Those modes with smaller amplitude cannot be unambiguously identified using this technique. In those cases the method described in the next section should be used.

#### 4. The excitation criterion applied to spectra observed at many stations

The spectra indicated as  $|A_r|$ ,  $|A_\theta|$  and  $|A_\phi|$  in Figs 12 and 13 are the absolute value of radial, co-latitudinal and azimuthal spectra respectively, summed over all stations. This summation does not help much to identify particular spectral peaks but enhances modes which are well excited, like those  ${}_0S$  peaks between 0.02 and 0.055 cycles/sec in  $|A_r|$  or the sequence of  ${}_0S$  peaks in the same spectrum between 0.07 and 0.008 cycles/sec. Similarly a clear sequence of equally spaced  ${}_3S$  peaks is observed in  $|A_\theta|$  between 0.0075 and 0.0086 cycles/sec.

$A_r$  in Figs 12 and 13 is the spectrum resulting from vectorial summation (phase and amplitude taken into account) of the same radial spectra used in  $|A_r|$ . The difference between  $A_r$  and  $|A_r|$  is striking, most of the peaks well developed in  $|A_r|$  have disappeared in  $A_r$ . This is due to the fact that for  $t = 0$  the phase of a peak at a given station can be 0 or  $\pi$  (see expression (1) and (2)). The phase of a given peak is  $\pi$  at some stations and 0 at others and when the spectra are vectorially added those peaks tend to cancel each other.  ${}_0S_{20}$  in  $A_r$  is a clear exception; it shows a large amplitude because it just happens that it has the same phase at almost all the stations.

It is possible to make the phase of a given mode the same in all the spectra by adding  $\pi$  to the observed spectra of those stations where its theoretical phase is  $\pi$  and leaving the remaining spectra unchanged. By doing that, the phase of the mode becomes equal to 0 at all stations and its peaks will add constructively when vectorially added. The result of such a summation after phase shift for the  ${}_0S_{20}$  mode is shown as  $A_r * P$  in Figs 12 and 13. Now  ${}_0S_{20}$  dominates the spectrum; most of the other peaks have almost disappeared because they have a different phase at different stations. Note that  ${}_0S_{20}$  has disappeared now. Some peaks, such as  ${}_0S_{22}$  at the right of  ${}_0S_{20}$ , have intermediate amplitudes because they have a spatial phase distribution close to that of  ${}_0S_{20}$ . Then it is clear that having a large number of spectra of stations all over the world and finding a suitable source and Earth model to predict the spectra at each station it is possible to filter out and unambiguously identify any peak if it is sufficiently well excited. Figs 14 to 28 show the result of application of this method to cases where the author believes that the identification is correct and the measured eigenfrequency is accurate. Doubtful cases are not shown. Particular comments on each mode identification are given in the Appendix. The display of detailed results has the purpose of allowing a critical analysis of these identifications when used for inversion.

Table 1 gives the eigenperiod measured in each case. The eigenfrequency was found by polynomial interpolation over 4 points of the discrete amplitude spectra. In order to enhance the signal to noise ratio the spectra at those stations where the theoretical amplitude of the mode under study was less than 0.5 times the average amplitude were discarded before summation. The resulting eigenperiods are an amplitude weighted average over all observing stations. This scheme has the effect of assigning weights proportional to the signal to noise ratio. Identifications only up to the sixth spheroidal overtone and third torsional overtone were attempted in this study.

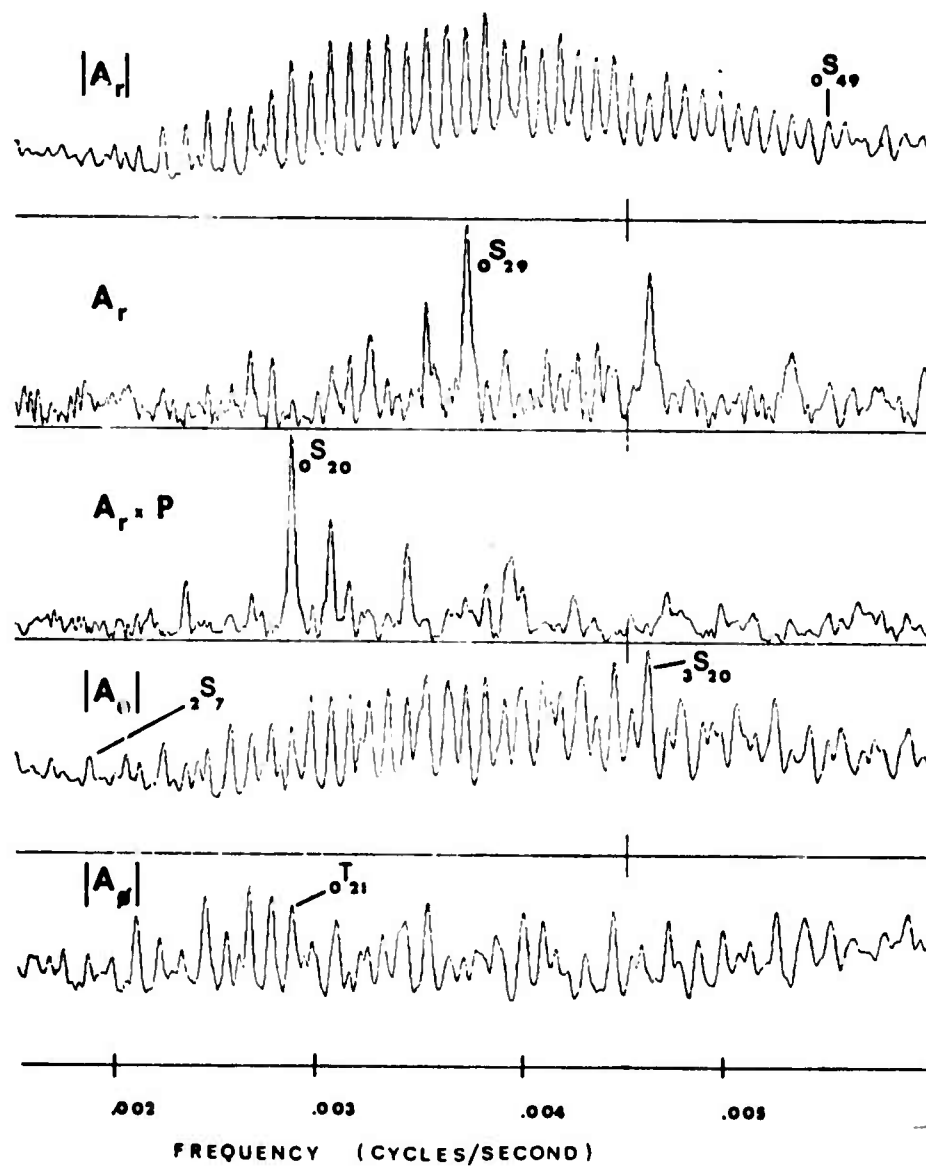


FIG. 12. Spectra resulting from summation of spectra observed at many stations over the Earth. The continuation of these spectra for smaller periods is shown in Fig. 13.

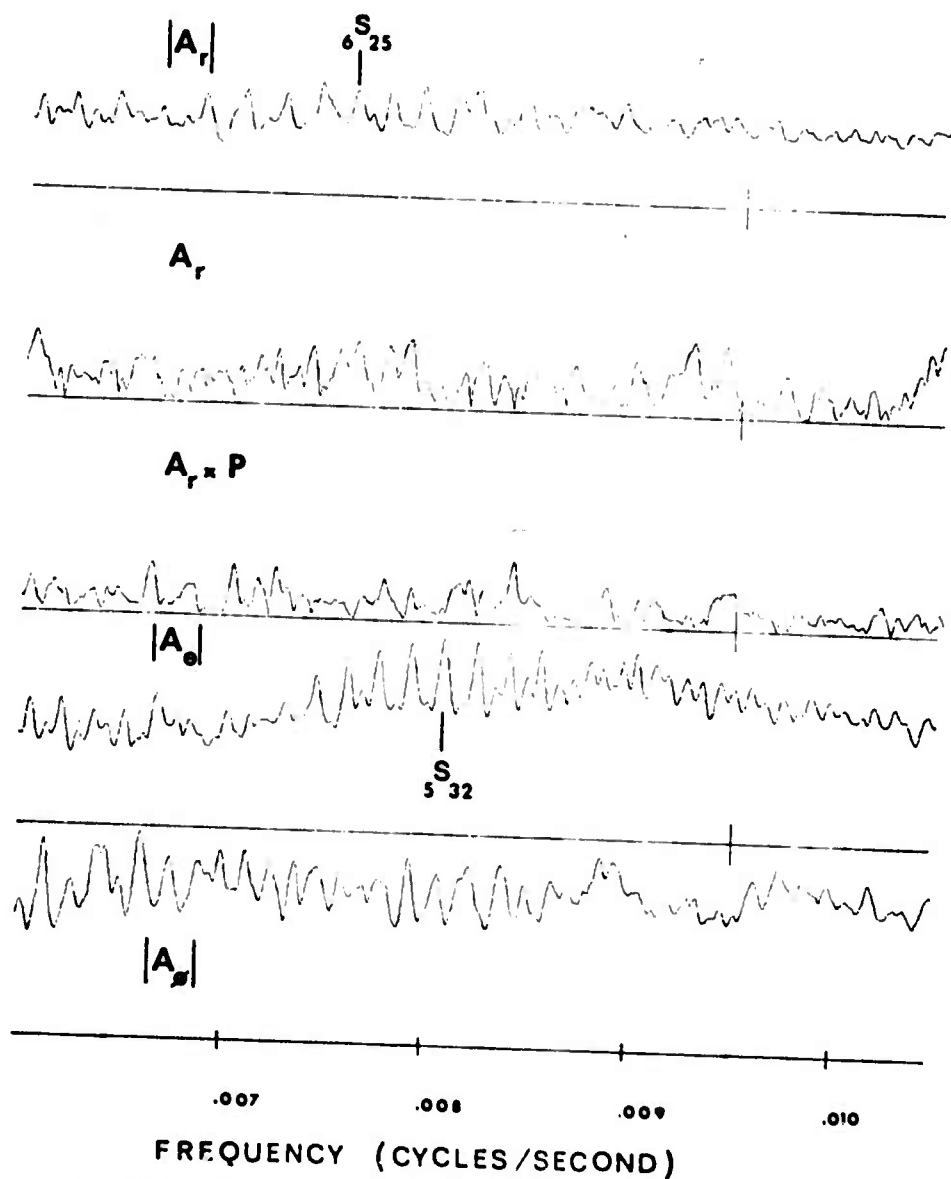


FIG. 13. Spectra resulting from summation of spectra observed at many stations over the Earth. They are a continuation of the spectra shown in Fig. 12.

Table 1

*Eigenperiods found using the excitation criterion. 'T' and 'S.D.' are the measured eigenperiods and the corresponding standard deviations in seconds. 'Delta' is the difference in seconds between the eigenperiod measured using all stations and the average over four subsets of stations.*

Observed eigenperiods

$n$	$T$	${}_0S_n$	S.D.	Delta	$n$	$T$	${}_1S_n$	S.D.	Delta
13	472.979		0.072	-0.000	23	229.347		0.057	0.006
14	448.201		0.074	0.013	29	190.894		0.115	0.000
15	426.056		0.050	0.000	36	161.353		0.087	-0.058
16	406.746		0.103	-0.022	38	154.758		0.079	0.040
17	389.134		0.118	0.007	39	151.475		0.001	-0.001
18	374.010		0.048	0.042	41	145.832		0.052	0.007
19	360.112		0.056	-0.011	42	143.047		0.121	-0.103
20	347.505		0.057	0.010	44	138.559		0.410	-0.048
21	335.811		0.100	-0.007	50	125.386		0.282	-0.118
22	325.059		0.027	-0.004	52	121.955		0.032	-0.013
23	315.213		0.116	-0.021	53	120.074		0.034	0.014
24	306.279		0.065	0.030	55	116.581		0.052	0.009
25	297.664		0.013	0.005					
26	289.601		0.026	-0.000					
27	282.181		0.054	0.005					
28	275.113		0.054	-0.024	$n$	$T$	${}_2S_n$	S.D.	Delta
29	268.436		0.043	0.009	6	595.011		0.756	0.039
30	262.060		0.098	0.013	7	535.260		0.990	0.279
31	255.952		0.110	0.009	10	415.916		0.770	-0.279
32	250.309		0.095	0.019	11	387.999		0.207	-0.082
33	244.919		0.133	0.030	12	365.230		0.248	0.009
34	239.585		0.041	0.012	13	343.219		0.357	-0.170
35	234.579		0.036	0.008	14	325.867		0.462	-0.042
36	229.806		0.038	-0.008	15	306.400		0.407	-0.336
37	225.215		0.036	-0.009	28	169.251		0.033	-0.002
38	220.742		0.015	-0.002	29	164.587		0.097	-0.043
39	216.478		0.033	0.001	30	160.553		0.031	0.010
40	212.381		0.035	-0.004	31	156.616		0.094	-0.043
41	208.347		0.029	0.003	32	152.684		0.037	0.010
42	204.579		0.022	0.001	33	149.169		0.155	0.094
43	200.927		0.031	0.004	35	142.614		0.074	-0.008
44	197.398		0.028	-0.000	36	139.507		0.041	0.002
45	193.875		0.041	-0.002	37	136.648		0.001	-0.000
46	190.624		0.042	0.015	38	133.858		0.104	0.086
47	187.258		0.093	-0.040	39	131.134		0.060	0.016
48	184.289		0.139	0.052	40	128.538		0.002	-0.001
49	181.002		0.021	0.004					
50	178.351		0.115	0.037					
51	175.267		0.075	-0.017	$n$	$T$	${}_3S_n$	S.D.	Delta
52	172.541		0.032	0.003	7	371.856		0.108	-0.075
53	170.089		0.011	-0.002	8	354.296		0.183	0.021
54	167.368		0.047	0.005	9	338.464		0.803	0.374
55	164.840		0.064	0.015	10	323.954		0.152	-0.057
56	162.482		0.130	0.033	11	310.149		0.260	0.174
57	160.265		0.066	0.076	12	297.475		0.075	-0.006
58	157.844		0.060	-0.006	13	284.982		0.050	-0.029
59	155.011		0.032	-0.002	14	273.351		0.098	-0.007
					15	262.467		0.091	0.031
$n$	$T$	${}_1S_n$	S.D.	Delta	16	251.984		0.043	-0.003
16	298.930		0.398	-0.047	17	242.443		0.125	-0.024
18	274.752		0.282	0.035	18	233.286		0.120	-0.077
21	245.017		0.278	0.004	19	224.910		0.121	-0.019

Table 1 (continued)

$n$	$T$	$s_{\bar{S}_n}$	$S.D.$	$\Delta$	$n$	$T$	$s_{\bar{S}_n}$	$S.D.$	$\Delta$
20	216.949	0.064	0.010		16	172.342	0.104	-0.079	
21	209.564	0.035	0.014		17	166.159	0.201	-0.026	
22	202.620	0.047	0.001		18	160.577	0.218	-0.183	
23	195.938	0.295	0.066		19	154.973	0.084	-0.063	
24	190.068	0.033	-0.011		20	150.090	0.045	0.030	
42	111.451	0.033	-0.001		21	145.756	0.017	0.000	
43	109.476	0.082	0.019		22	141.909	0.031	-0.007	
44	107.776	0.032	0.010		23	138.329	0.053	0.049	
45	105.976	0.094	0.049		24	134.794	0.053	-0.020	
46	104.197	0.101	-0.070		25	131.784	0.034	-0.018	
47	102.585	0.074	0.029		26	128.697	0.101	-0.072	
48	101.141	0.032	0.008		27	125.951	0.036	0.007	
49	99.462	0.084	0.059		28	123.514	0.080	0.001	
50	98.014	0.020	-0.006		29	121.043	0.019	-0.015	
51	96.439	0.069	-0.013		32	114.452	0.073	0.032	
52	94.961	0.052	-0.036						
53	93.725	0.193	0.161						
54	92.336	0.184	-0.013						
56	90.103	0.001	-0.000						
57	88.882	0.000	0.000						
58	87.654	0.031	-0.011						
$n$	$T$	$s_{\bar{S}_n}$	$S.D.$	$\Delta$	$n$	$T$	$s_{\bar{T}_n}$	$S.D.$	$\Delta$
32	135.649	0.071	-0.001		11	574.487	0.181	0.041	
33	132.825	0.102	0.011		12	539.946	1.233	0.155	
34	129.931	0.063	-0.014		13	506.832	0.306	0.183	
35	127.243	0.030	0.007		14	477.511	0.281	0.141	
36	124.668	0.045	0.006		15	452.933	0.220	-0.018	
37	122.242	0.019	-0.001		16	431.229	0.590	-0.070	
38	119.843	0.035	0.009		17	410.350	0.210	-0.095	
39	117.608	0.035	0.025		18	392.354	0.259	0.098	
40	115.436	0.077	0.019		19	374.555	1.086	-0.738	
41	113.375	0.021	0.001		20	358.718	0.174	-0.033	
					21	346.142	0.286	-0.028	
					22	332.855	0.251	0.110	
					23	321.953	0.351	0.002	
					24	310.362	0.322	-0.077	
					25	300.186	0.260	-0.022	
					26	290.660	0.079	-0.047	
					27	281.867	0.321	0.198	
					29	264.934	0.178	-0.024	
					30	257.830	0.325	0.083	
$n$	$T$	$s_{\bar{S}_n}$	$S.D.$	$\Delta$	$n$	$T$	$s_{\bar{T}_n}$	$S.D.$	$\Delta$
24	147.027	0.028	0.005		7	475.191	0.617	-0.096	
25	143.594	0.019	-0.004		8	438.962	0.393	0.067	
26	140.266	0.066	0.008		9	407.752	0.797	-0.307	
27	137.122	0.047	0.023		10	381.228	0.504	0.098	
28	134.064	0.057	-0.005		11	359.077	0.486	-0.006	
29	131.176	0.020	-0.010		12	339.239	0.151	0.172	
30	128.477	0.061	-0.030		13	322.837	0.398	-0.075	
31	125.881	0.056	-0.011		14	306.996	0.197	0.009	
32	123.433	0.053	-0.026		15	293.364	0.074	0.006	
33	121.030	0.017	-0.006		16	280.515	0.151	-0.054	
34	118.768	0.020	-0.000		17	269.202	0.253	0.113	
35	116.633	0.040	0.006		18	259.092	0.343	0.138	
36	114.527	0.038	-0.002		19	249.158	0.155	0.044	
37	112.543	0.017	-0.009		20	240.977	0.224	0.048	
38	110.590	0.000	0.000		21	232.529	0.112	-0.001	
39	108.665	0.001	0.000		22	225.190	0.052	-0.010	
40	106.850	0.001	0.000		23	218.379	0.141	-0.011	
41	105.051	0.026	0.015		24	211.948	0.024	0.007	
42	103.354	0.002	0.000		25	205.853	0.103	0.034	
43	101.707	0.052	0.032		26	200.270	0.040	0.001	
44	100.079	0.001	0.000						
46	97.040	0.016	0.009						

5

e

g

s

fi

2

s

s

t

f

r

c

e

d

c

s

f

s

v

t

c

t

(

r

r

s

s

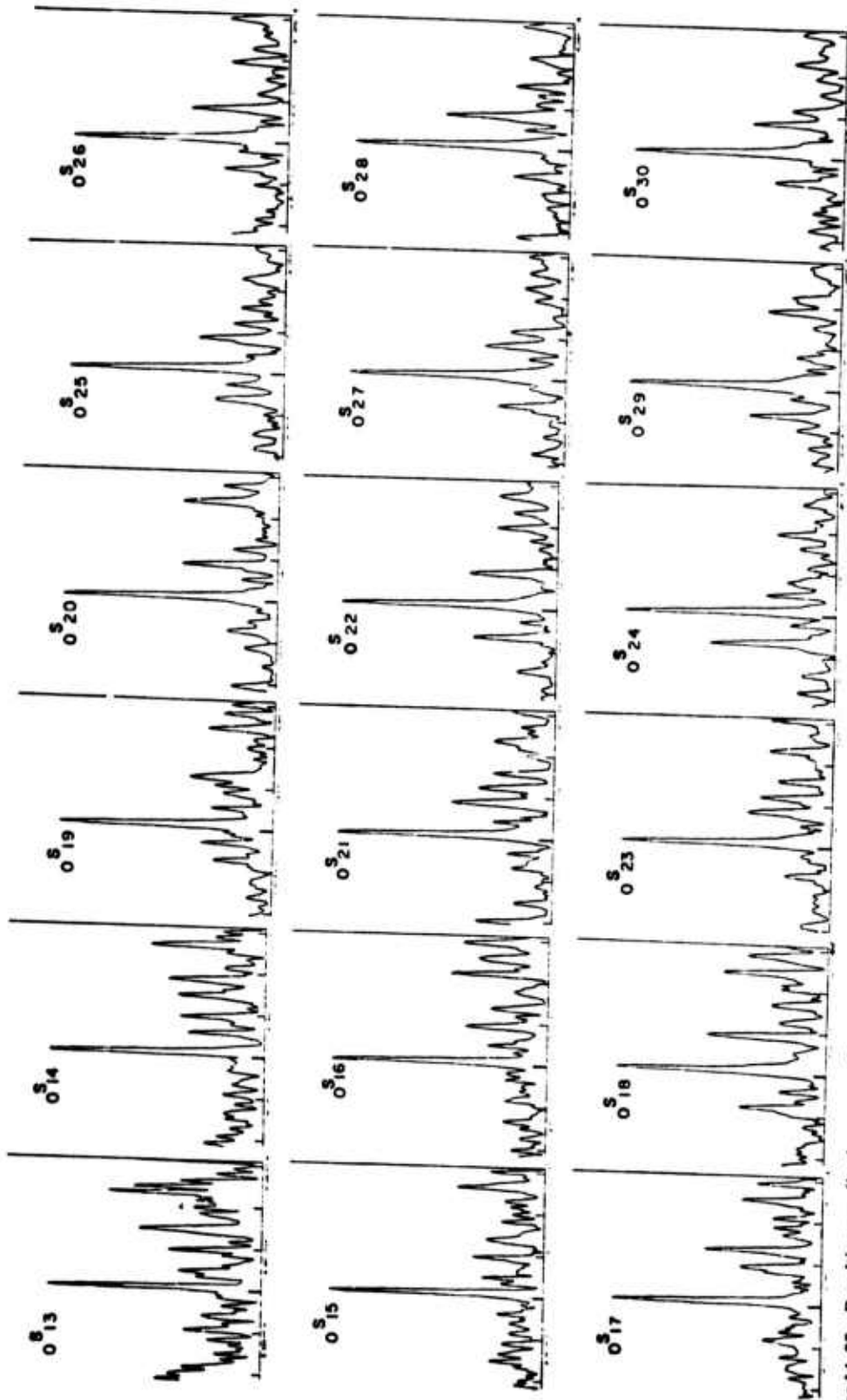
Table 1 (continued)

<i>n</i>	<i>T</i>	<sup>1</sup> <i>T<sub>e</sub></i>	<i>S.D.</i>	<i>Delta</i>	<i>n</i>	<i>T</i>	<sup>2</sup> <i>T<sub>e</sub></i>	<i>S.D.</i>	<i>Delta</i>
27	194.943		0.022	-0.016	25	171.123		0.126	-0.033
28	190.085		0.109	-0.035	27	162.581		0.138	0.000
29	185.338		0.096	-0.020	28	158.409		0.150	-0.037
31	176.849		0.130	0.053	29	154.571		0.049	0.005
32	173.027		0.324	-0.205	32	144.201		0.210	0.016
33	169.156		0.041	0.019	37	130.406		0.268	-0.172
34	165.715		0.085	0.064	38	128.168		0.099	0.055
35	162.356		0.032	-0.008	41	121.571		0.048	-0.007
36	159.113		0.022	0.018	42	119.330		0.172	0.177
37	155.982		0.034	0.013					
38	153.165		0.115	-0.060					
39	150.253		0.056	0.008					
40	147.681		0.007	0.007					
41	145.121		0.049	0.006	<i>n</i>	<i>T</i>	<sup>2</sup> <i>T<sub>e</sub></i>	<i>S.D.</i>	<i>Delta</i>
42	142.661		0.052	0.010	17	189.973		0.247	-0.154
43	140.230		0.111	0.006	19	178.104		0.080	-0.016
44	137.960		0.082	0.021	24	154.809		0.184	-0.110
45	135.638		0.330	-0.235	25	150.663		0.047	-0.025
47	131.592		0.222	-0.101	26	146.936		0.310	-0.189
49	127.651		0.021	-0.012	28	140.390		0.099	-0.067
51	124.127		0.539	-0.411	29	137.193		0.067	0.020
54	119.127		0.050	-0.004					

### 5. Accuracy of the measured eigenperiods

The error in the eigenperiods determined by vectorial summation of spectra was estimated as follows. The stations were grouped into four subsets based on the geographical location with respect to the epicentre. The first subset includes those stations located at epicentral distance between  $0^\circ$  and  $5^\circ$ ,  $10^\circ$  and  $15^\circ$ ,  $20^\circ$  and  $25^\circ$  and so on. The second subset includes the remaining stations. The third subset was formed with those stations located at azimuth between  $0^\circ$  and  $5^\circ$ ,  $10^\circ$  and  $15^\circ$ ,  $20^\circ$  and  $25^\circ$  and so on. The fourth subset includes all the stations not contained in the third subset. This particular way of grouping stations has the characteristic that each subset samples approximately the same regions of the Earth. Therefore it is expected that the bias introduced by the different combination of stations on the measured eigenperiods may be minimized. The fluctuations in the eigenperiods found for each subset results primarily from errors due to noise, data handling, and an unknown effect of combining different station data. The excitation criterion was applied separately to each one of these subsets and the eigenperiods were measured. In general, the difference in eigenperiods among subsets is very small and indicates that the excitation criterion renders stable results. In many cases the summation of only 20 spectra gave stable estimates of overtone eigenperiods. The difference between the average eigenperiods over the four subsets and the eigenperiod found from a combination of all stations is given in Table 1. The standard deviation of the eigenperiods determined using all stations was estimated dividing the standard deviation found for the subsets by  $\sqrt{2}$ , as each subset contains half the total number of stations. The standard deviation of each measurement is listed in Table 1. Those standard deviations are of the same order of the SEM found for the Alaskan earthquake free oscillations (Dziewonski & Gilbert 1972a) for those modes identified in both cases. This agreement indicates that summing vectorially the spectra or taking the average over measurements at single stations gives results of a similar accuracy.

The average standard deviation for  ${}_0S_{13}$  to  ${}_0S_{50}$  eigenperiods measured at different subsets is 0.025 per cent. As each subset samples the same region of the Earth, the average 0.025 per cent may be considered the minimum expected bias introduced by



FIGS 14-28. Resulting amplitude spectra after vectorial summation. The amplitude is plotted on a linear scale. The larger ticks on the frequency axis indicate the theoretical eigenfrequency for each mode corresponding to the HB1-6 Earth model.

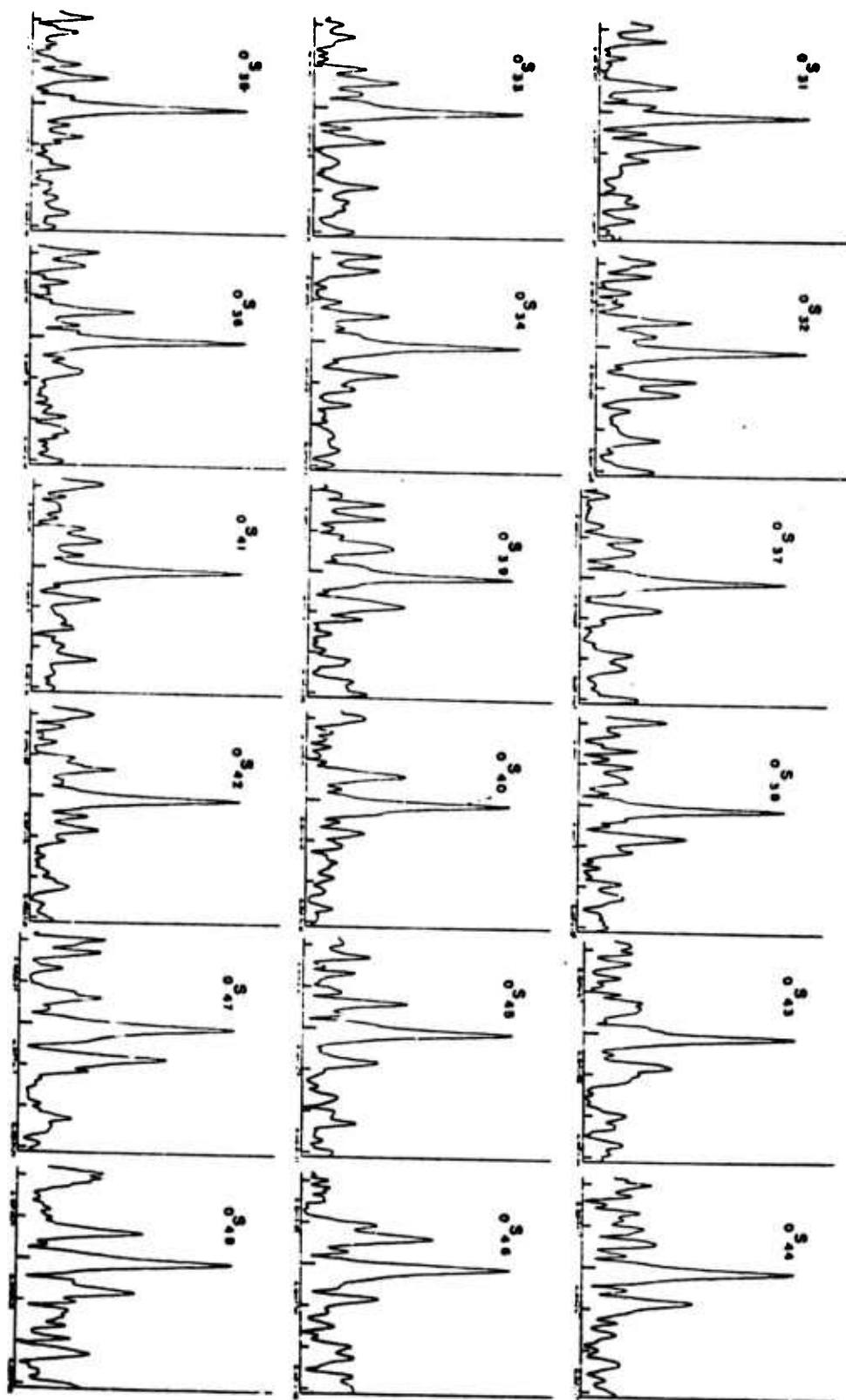


FIG. 15

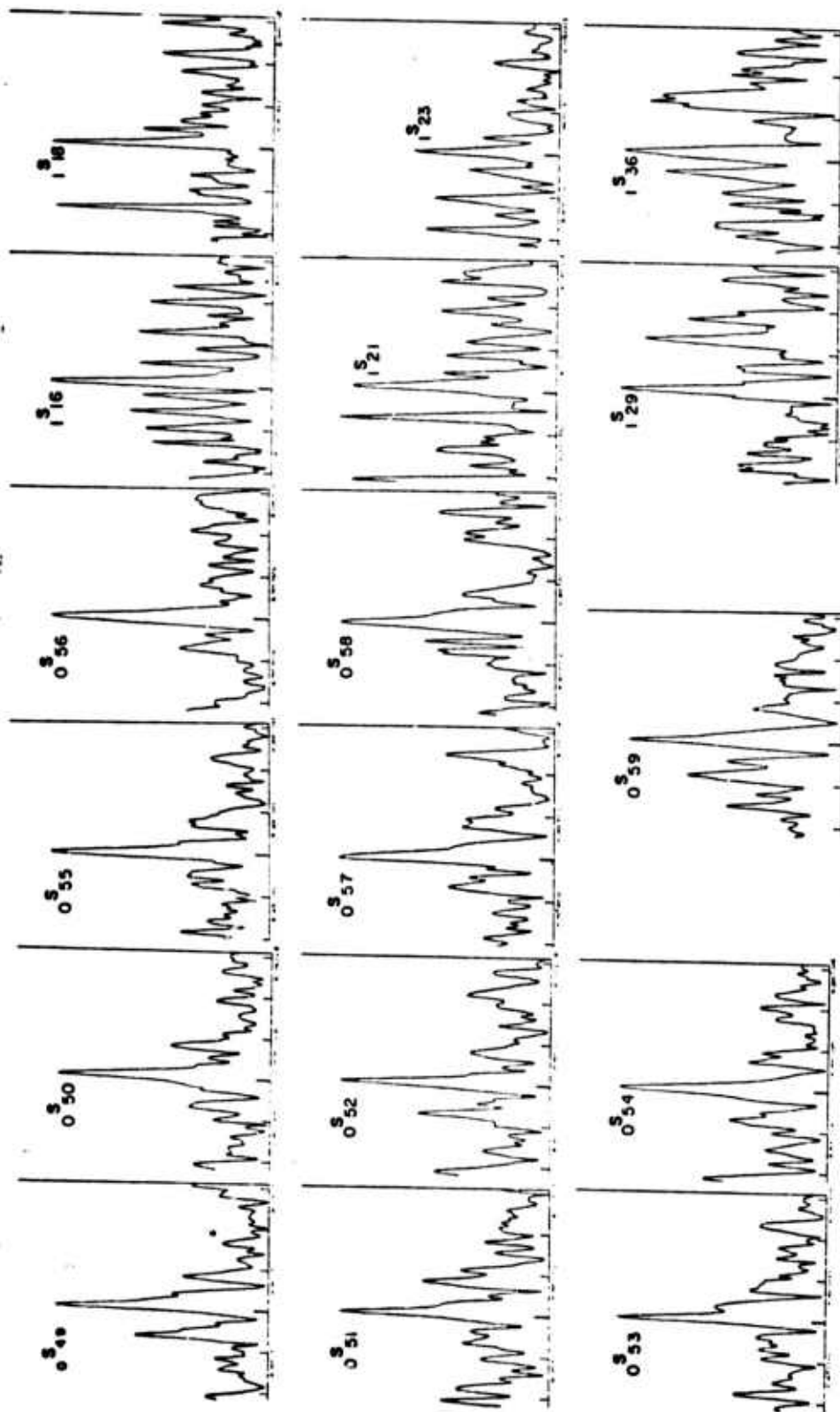
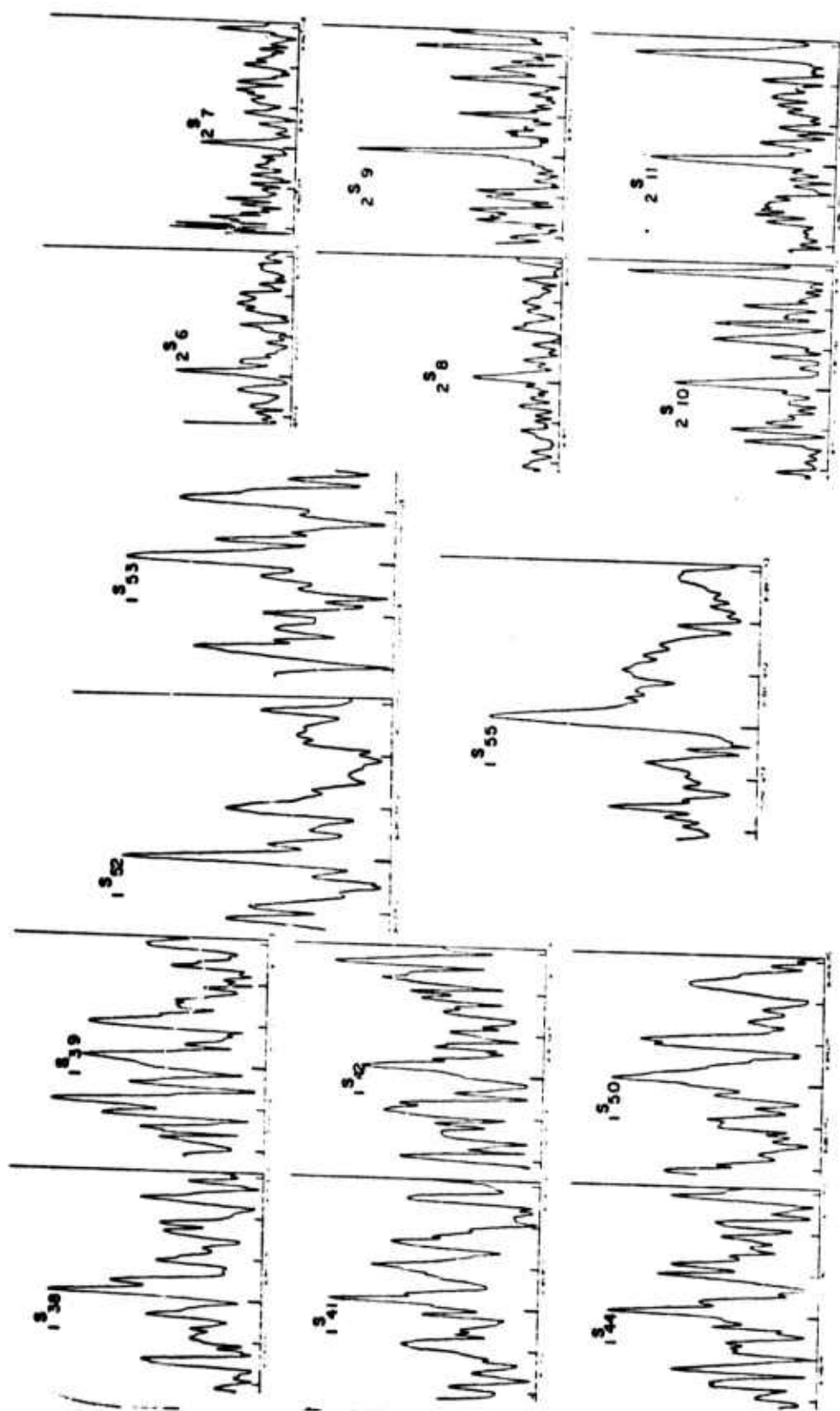


FIG. 16



**FIG. 17**

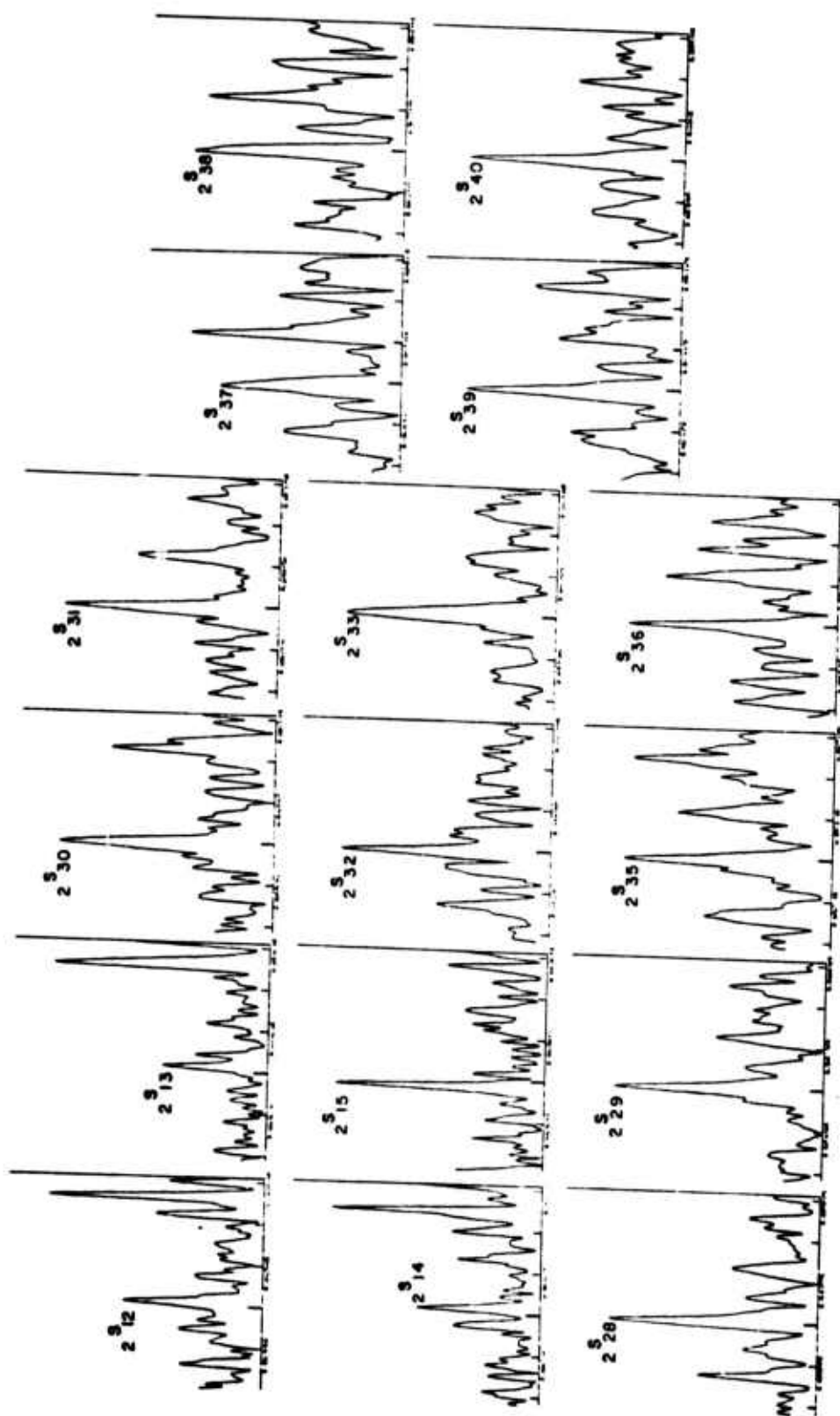


FIG. 18

Identification of free oscillation spectral peaks

305

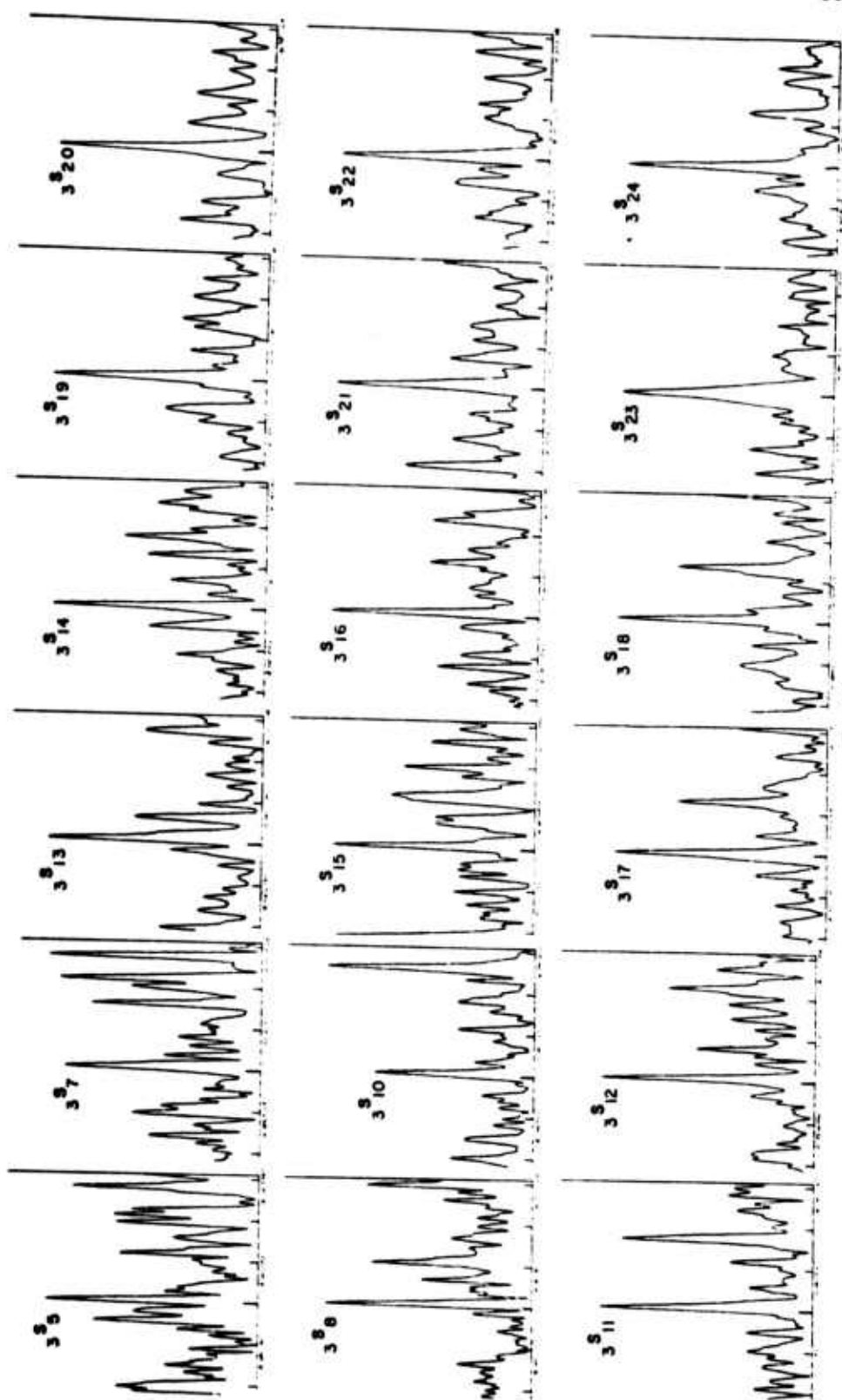


FIG. 19

306

J. A. Mendiguren

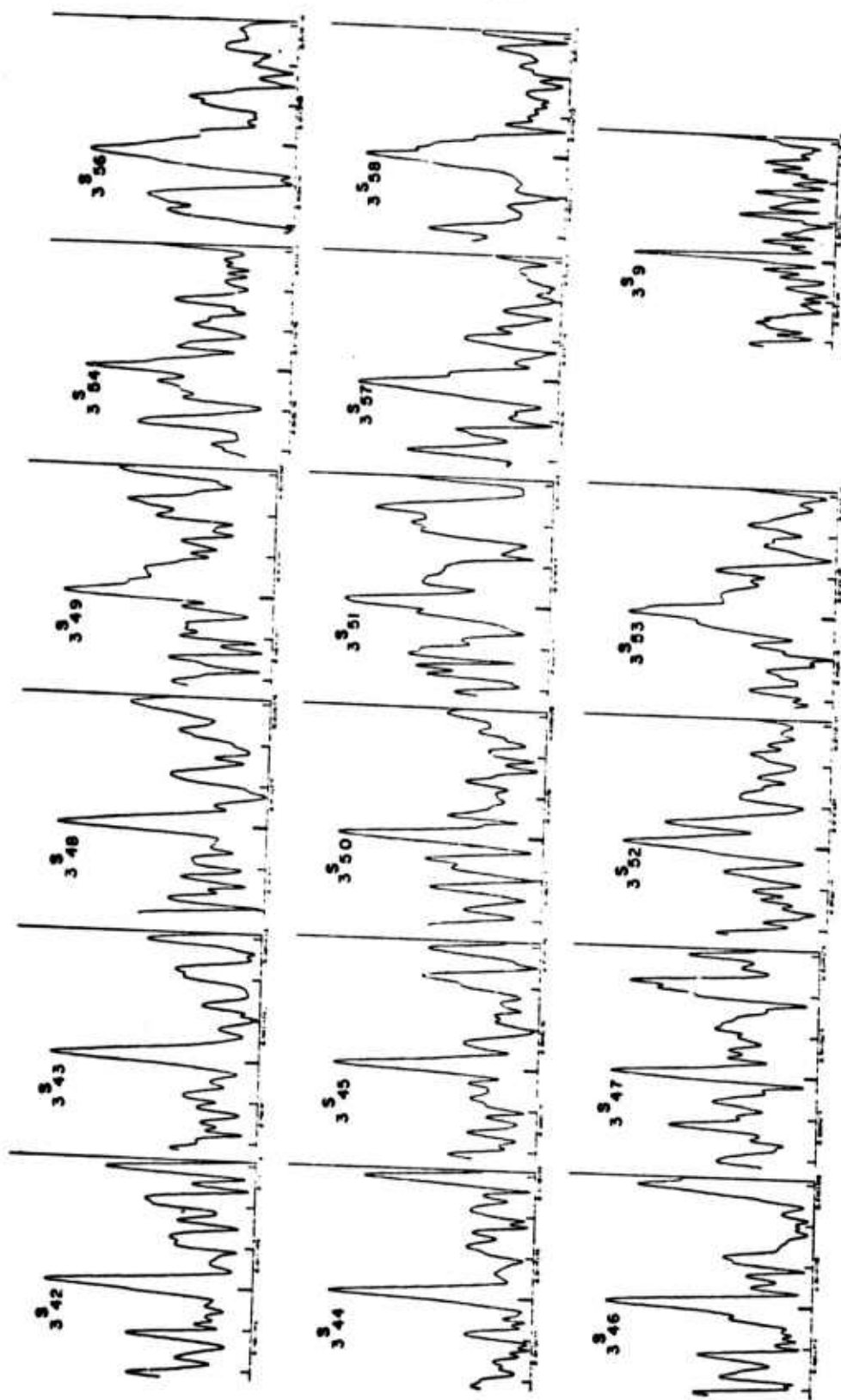


FIG. 20

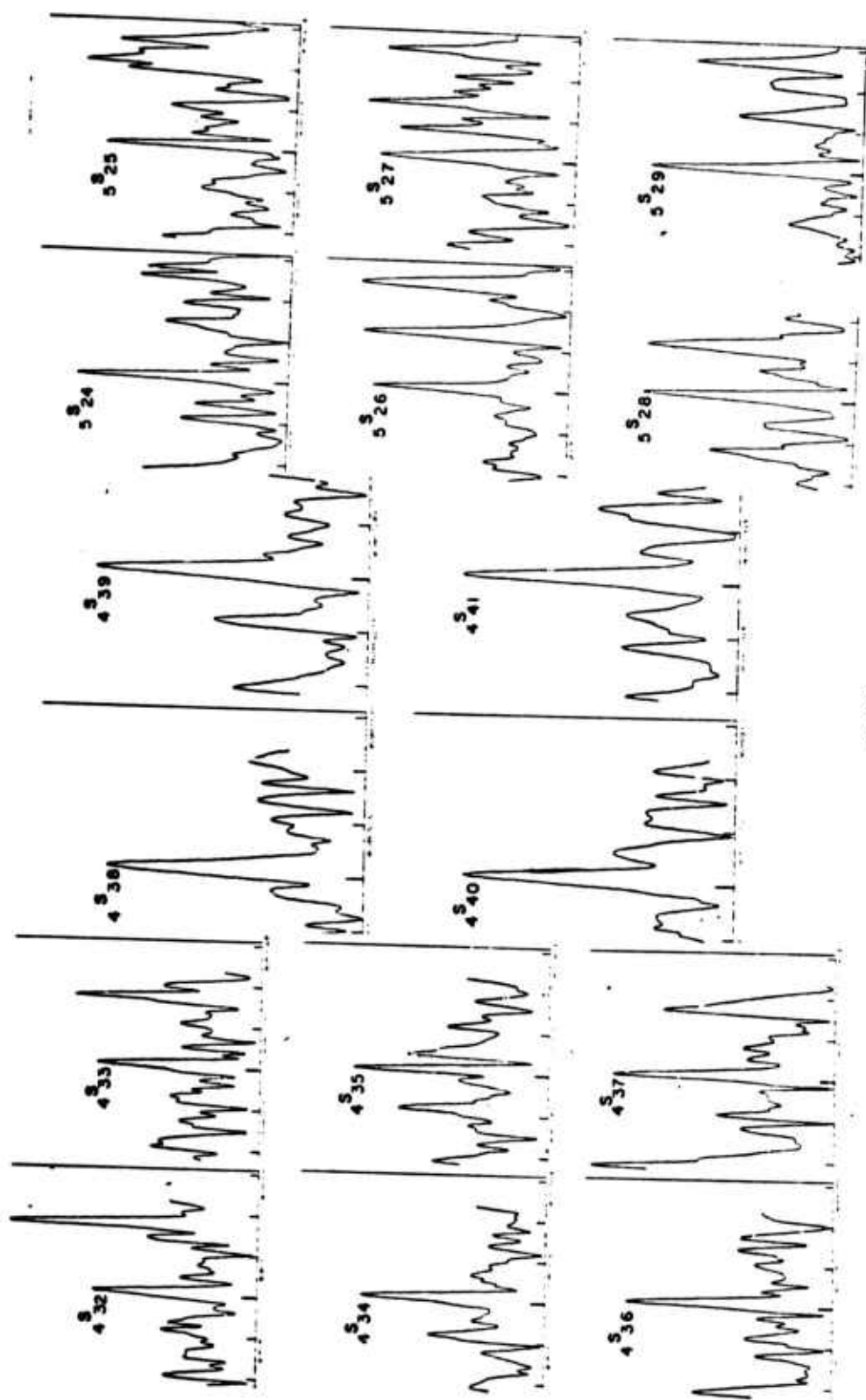


FIG. 21

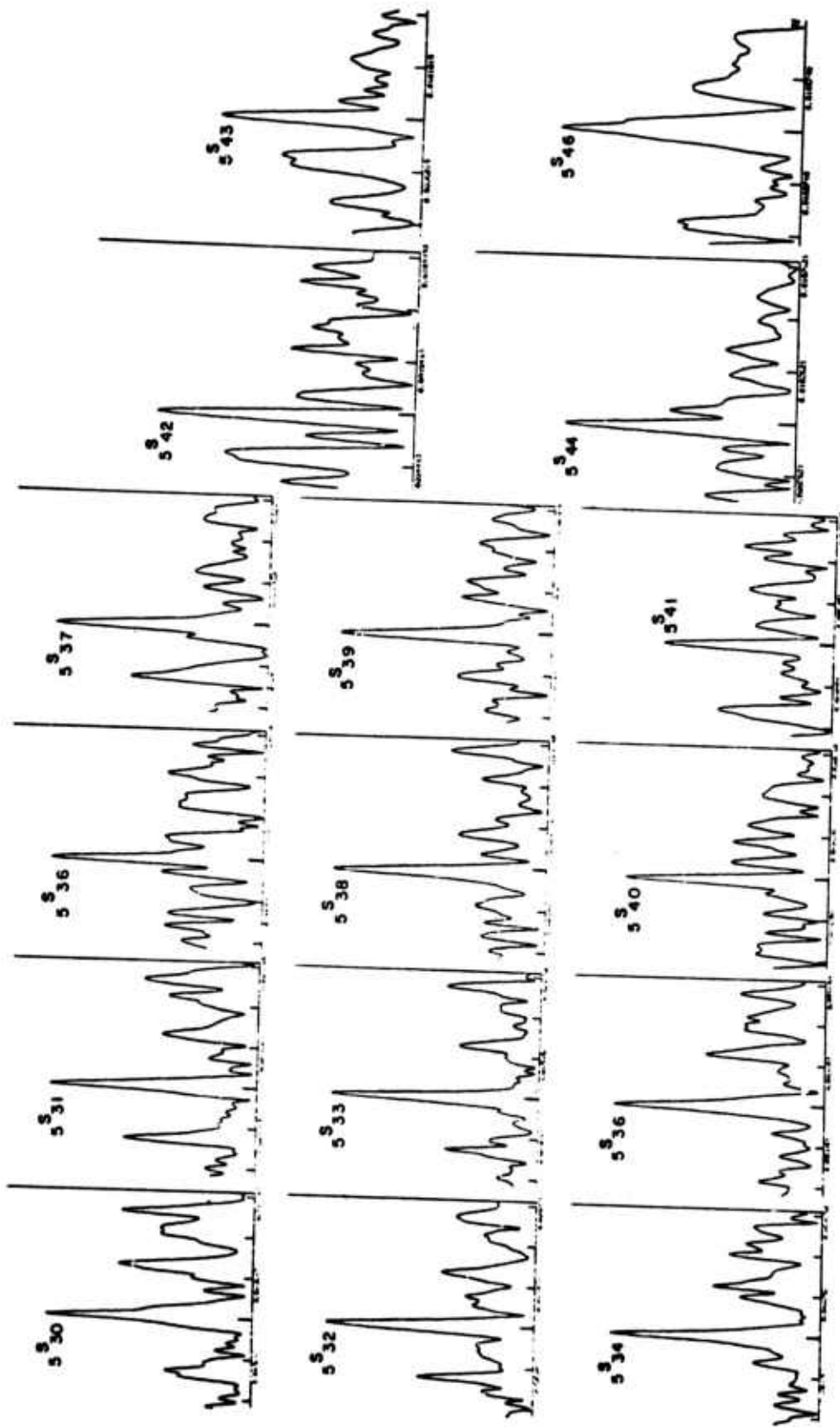


FIG. 22

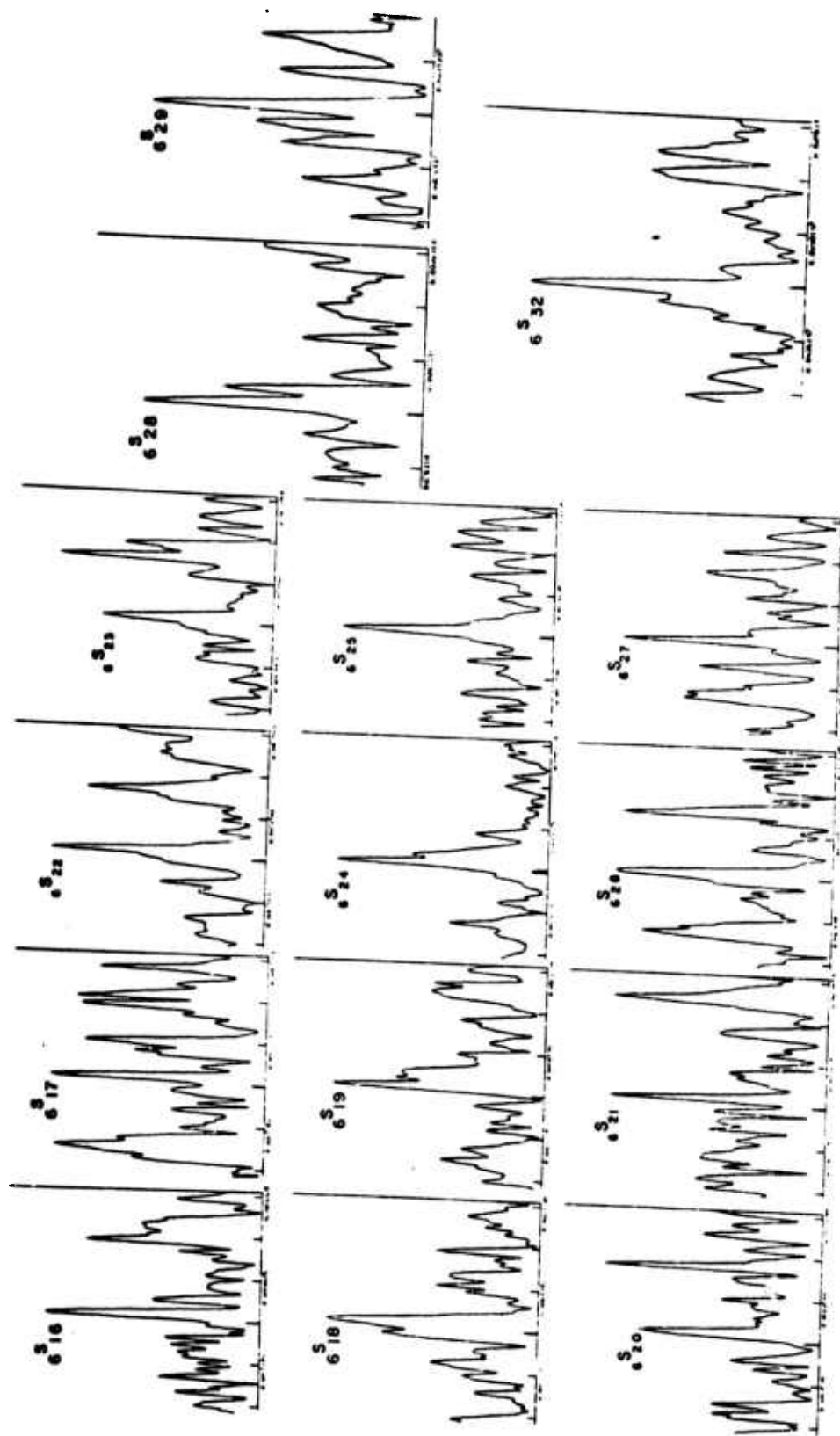


FIG. 23

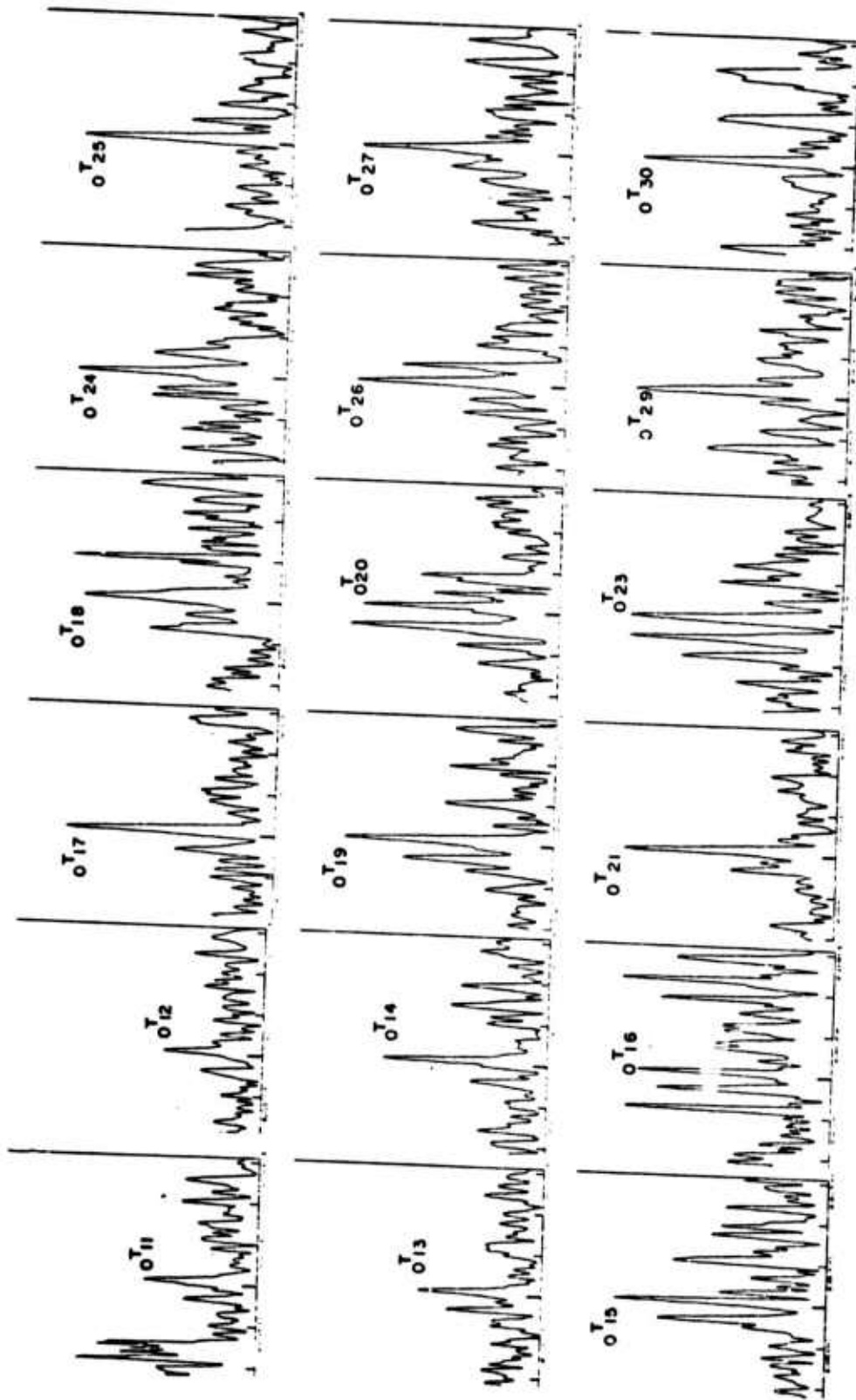


FIG. 24

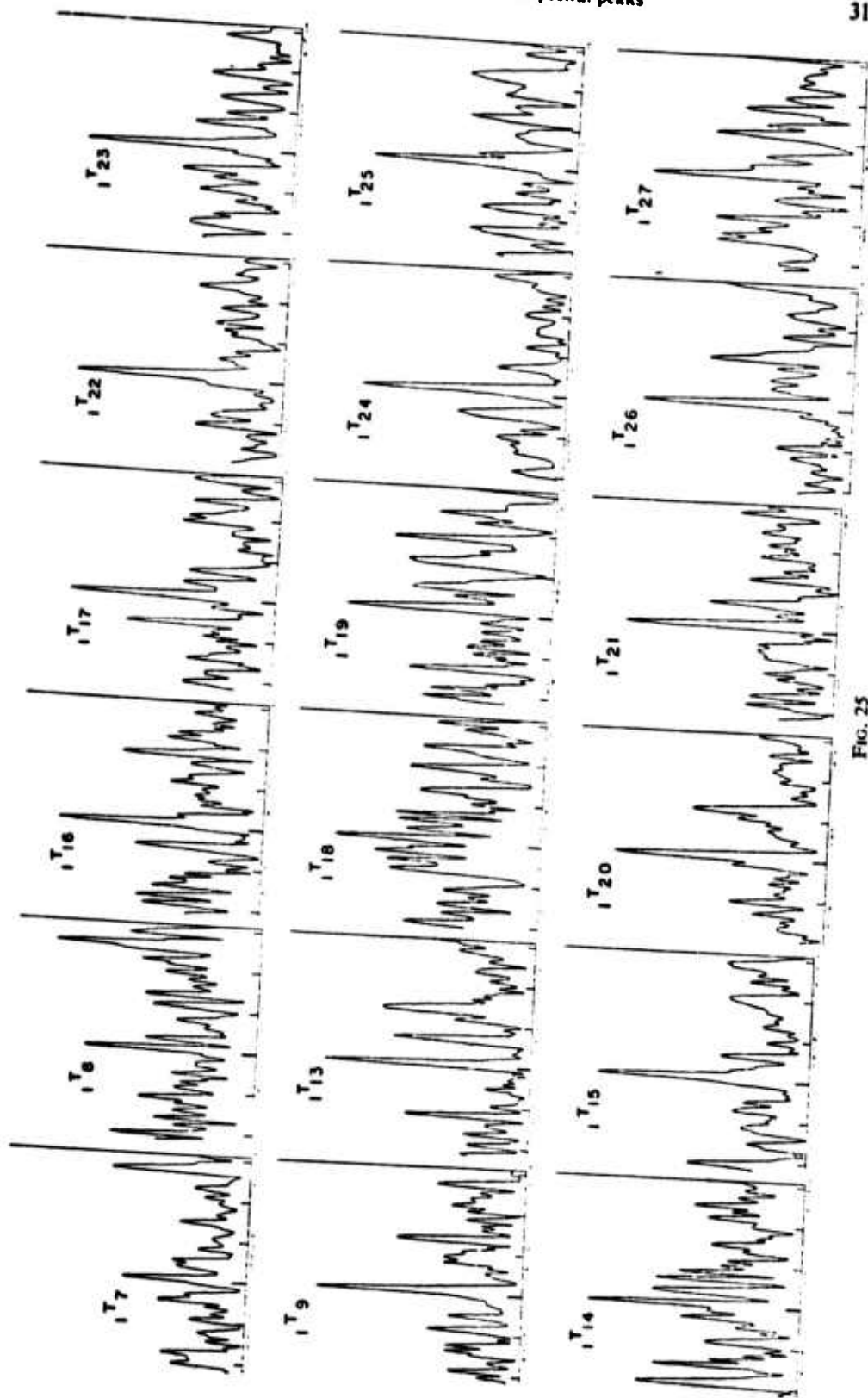


FIG. 25

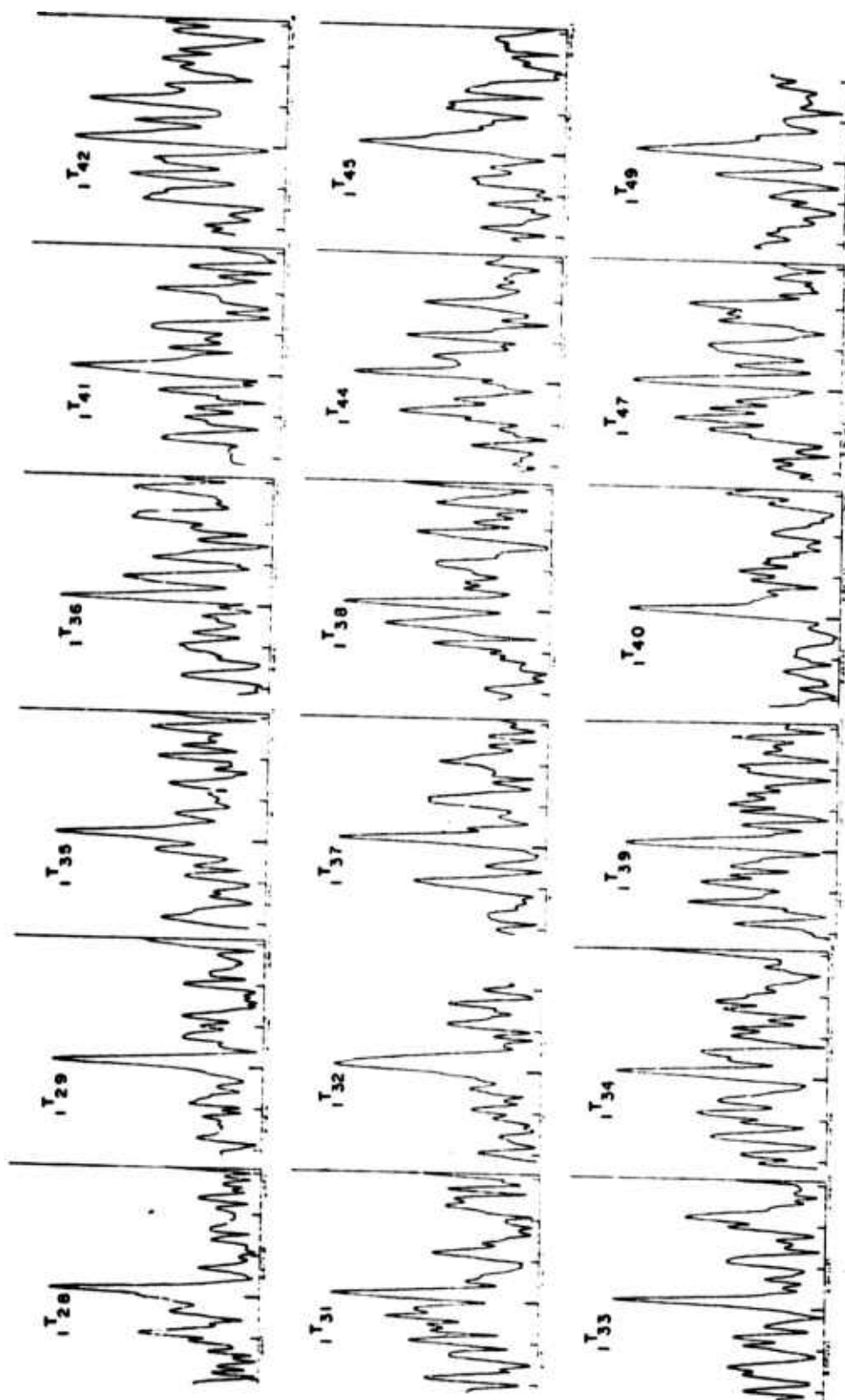


FIG. 26

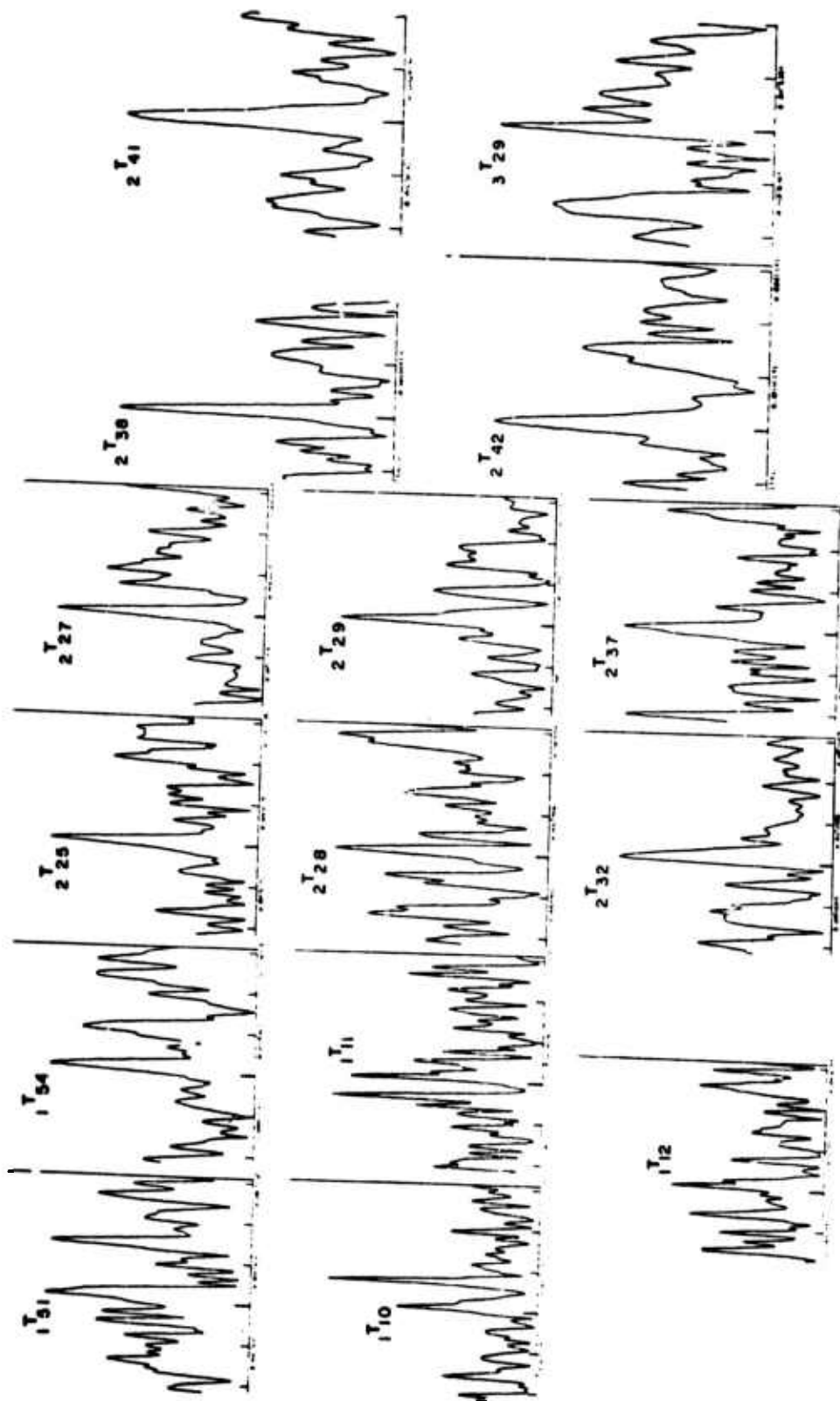


FIG. 27

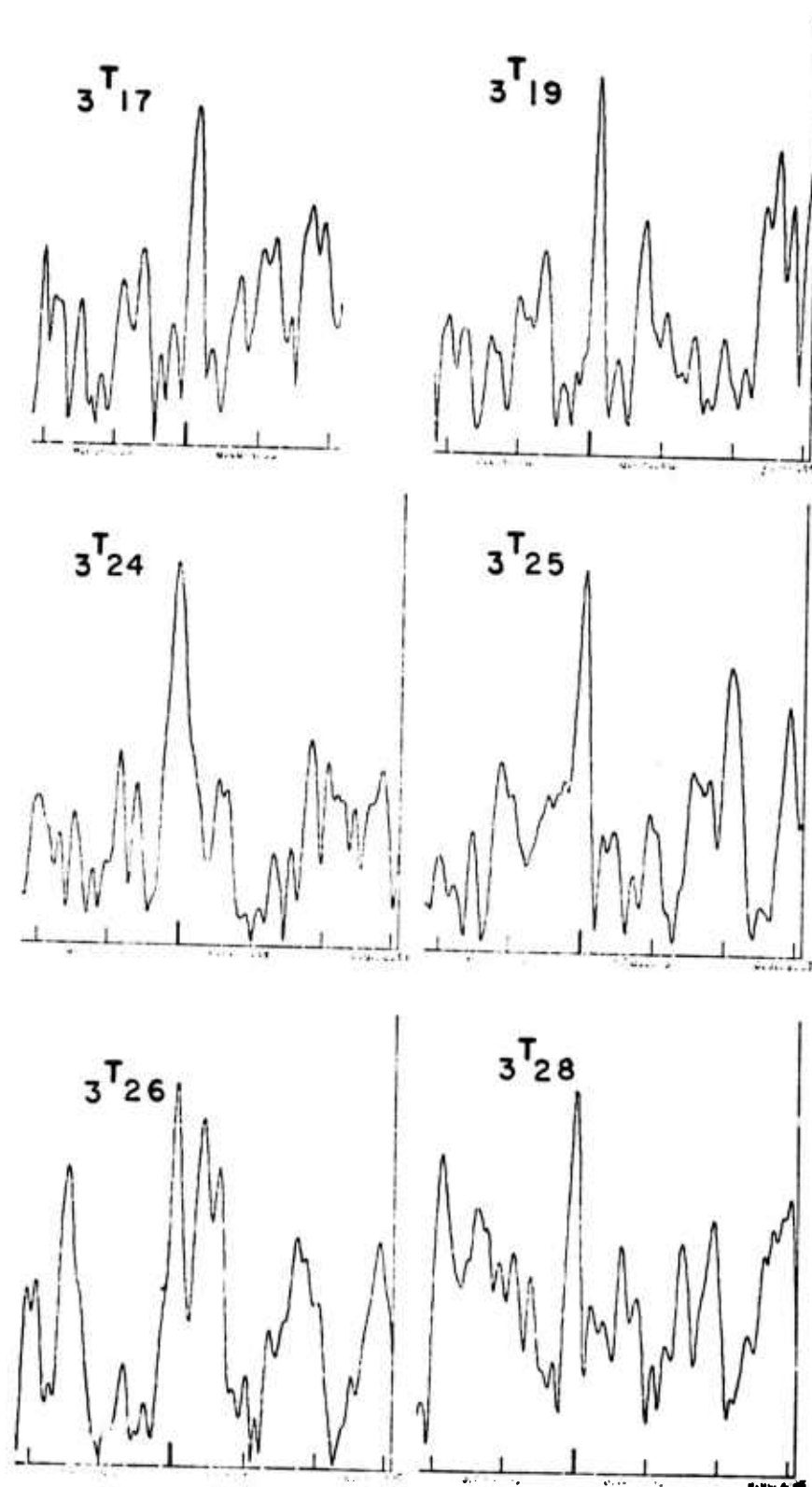


FIG. 28

the arbitrary selection of stations and epicentre location for any  ${}_0S_n$  eigenperiod determination.

Figs 29 and 30 show the  ${}_0S_n$  and  ${}_0T_n$  eigenperiods measured for the Alaskan and Colombian events, taking the average eigenperiods published by Derr (1969) as reference.

The mean difference between Derr's eigenperiods and the Colombian data in the range from  ${}_0S_{13}$  to  ${}_0S_{40}$  is +0.030 per cent while the mean difference between Derr's averages and the Alaskan data is 0.058 per cent. The Colombian data is closer to Derr's averages than the Alaskan data, but while the lines for the Alaskan and Colombian shock are roughly parallel to each other, they show a more erratic departure from Derr's averages. This demonstrates consistency of data obtained for the Alaskan and Colombian shock and also suggests that the Derr's data have large scattering. The systematic difference between the eigenperiods on the Alaskan and Colombian shocks in the range from  ${}_0S_{13}$  to  ${}_0S_{40}$  is 0.045 per cent. It is smaller than the standard deviation of the measurements at individual stations but it is larger than the standard error of the mean. This indicates that the heterogeneities and anisotropies of the Earth are such that for a given epicentre and the present distribution of stations the average eigenfrequency measured over all stations may differ from the degenerate value of the ideal average laterally homogeneous Earth by an amount larger than the SEM. The full circles in Fig. 29 indicate the eigenperiods measured for the Colombian shock on the co-latitudinal component. The mean deviation between the vertical and co-latitudinal measurements is 0.023 per cent. This difference can be attributed to the different combination of stations used in each case. As shown in Fig. 3 for KOD the excitation of the vertical and horizontal component are different for each mode at a given station. The horizontal spectra were not combined with the vertical spectra because while  ${}_0S_n$  modes dominate the vertical component they are more contaminated by other modes in the horizontal component, see  $A_r$  and  $A_\theta$  in Fig. 12. If we had combined both data the systematic deviation between the Colombian and Alaskan measurements would have been reduced to about 0.035 per cent but it still would be significant.

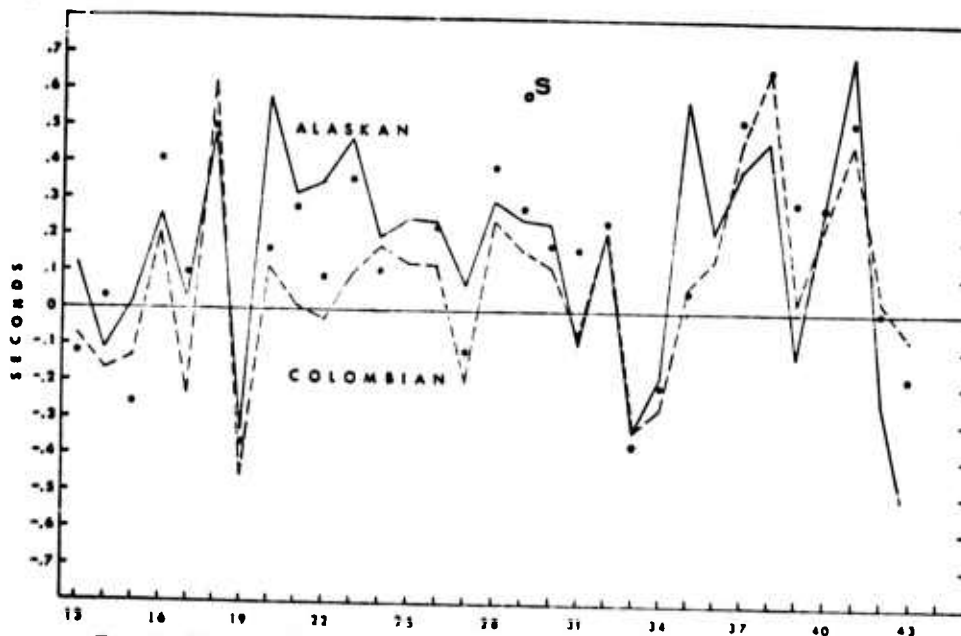


FIG. 29. Eigenperiods of  ${}_0S_n$  modes measured for the Alaskan and Colombian shock plotted as a function of  $n$ . The 0 reference line corresponds to the average eigenperiods published by Derr (1969). Full circles indicate eigenperiods measured for the Colombian shock on the co-latitudinal component.

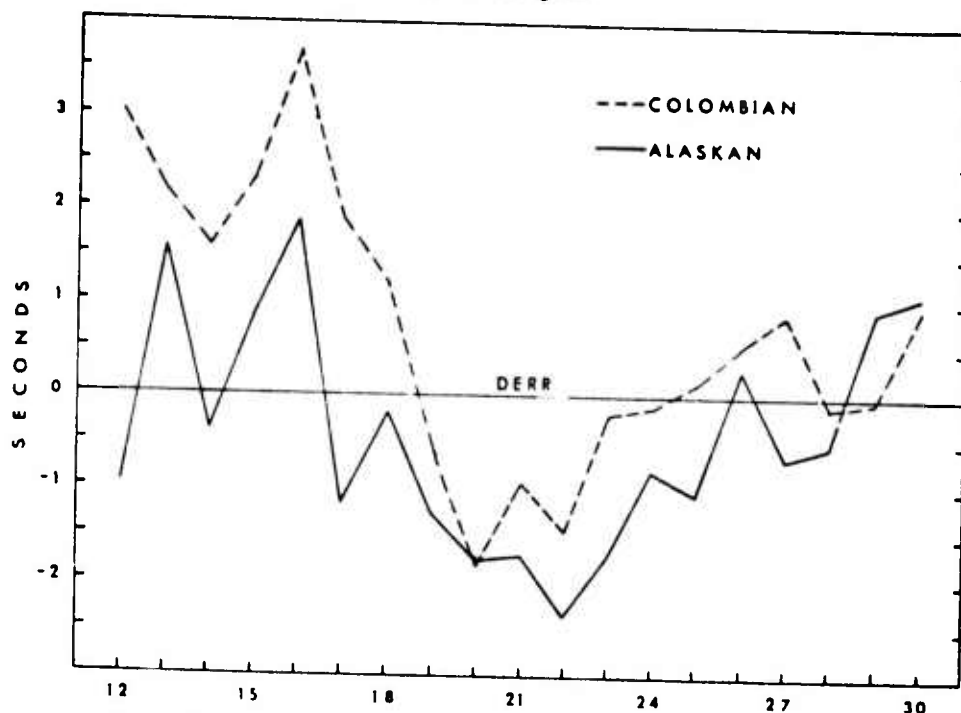


FIG. 30. Eigenperiods of  ${}_0T_n$  modes measured for the Alaskan and Colombian shocks plotted as a function of  $n$ . The 0 reference line corresponds to the average eigenperiods published by Deir (1969).

It is remarkable that the difference in eigenperiods have different sign for  ${}_0T_n$  and  ${}_0S_n$ . It is also different in magnitude. The systematic difference in  ${}_0T_n$  eigenperiods in the range from  ${}_0T_{13}$  to  ${}_0T_{30}$  is 0.321 per cent or 7 times larger than the difference for  ${}_0S_n$  eigenperiods. The Colombian data shows faster Rayleigh waves and slower Love waves as compared with the Alaskan shock. A similar type of observation was made by Aki (1966) who found a difference in phase velocity of 0.4 per cent for Love waves at 200 s measured over many great circle paths for the Niigata 1964 event and over paths through Pasadena (Toksöz & Anderson 1963).

Only with overtones for  ${}_3S_n$  modes are there sufficient data to compare Alaskan and Colombian measurements. The Colombian eigenperiods  ${}_3S_7$  to  ${}_3S_{11}$  are consistently smaller than the Alaskan. The average difference is 0.115 per cent while 0.090 per cent is the average S.D. of the measurements.

## 6. The excitation criterion, general remarks

The success of the excitation criterion depends on how well we can predict theoretically the free oscillation spectra at a given station. Since the theoretical spectra are derived by assuming an Earth and source model the question is how critical is the choice of those models for a successful peak identification.

In the case of the free oscillations identified in this paper the change of model from HB1-6 (Haddon & Bullen 1969) to the 5.08 M (Press 1968; Kanamori 1970) did not introduce any significant difference in the results. The main features of the theoretical spectra at each station remained the same, and the only effect of changing the Earth model was to shift the eigenperiods and slightly change the amplitudes. This result is due to the fact that a change in Earth model does not change drastically the shape of the eigenfunctions, at least for modes of low radial order. For higher overtones the shape of the eigenfunctions becomes more structure dependent and in those

cases clearer identification should be expected when using a more accurate Earth model. But in general, the excitation criterion is not critically dependent on the assumed Earth model.

A more serious difficulty is posed by the lateral heterogeneities of the real Earth. Mendiguren (1972a) observed that a laterally homogeneous Earth model is adequate to predict the spectra of modes with long wavelengths. But for shorter wavelengths the lateral heterogeneities cause an increasing disagreement between theoretical and observed spectra and finally at some critical frequency the predicted spectra do not resemble the observed ones. That critical wavelength is different for different modes, and depends on the depth of penetration in each case. For example for  ${}_0T$  modes the critical period is around 300 s while for  ${}_0S$  modes it is around 180 s (Mendiguren 1972a). In general those modes with much of their energy in the upper 300 km of the Earth are more affected than those modes penetrating deeper. Therefore for each particular mode there is a critical frequency beyond which it is not possible to predict adequately the spectra assuming a laterally homogeneous Earth and hence the excitation criterion cannot be applied.

The assumption of a point source model in the excitation criterion scheme used for the Colombian earthquake was adequate because the linear dimension of the source were smaller than 100 km (Mendiguren 1972a) or about 10 times smaller than the shortest wavelength of the identified modes. For shocks associated with larger fault dimensions the source finiteness should be taken into consideration (e.g. Press *et al.* 1969) when computing the theoretical spectra and the phase correction before vectorial summation.

The complications introduced by the presence of aftershocks in the study of free oscillations have been overestimated in the past (K. Aki, private communication). Earlier it was argued that as the amplitude goes like the square root of the energy the amplitude of long period oscillations should be proportional to  $\sqrt{10^{M_s}}$  where  $M_s$  is the surface wave magnitude. But in fact the amplitude at long periods is proportional to the seismic moment (Aki 1967) or proportional to  $10^{M_s}$ .

Anyhow, when applying the excitation criterion in the presence of large aftershocks, their effect on the observed spectra could be taken into account if their source mechanism and seismic moment were known. The predicted spectra would be in this case the result of summing the spectra for the main event and aftershocks. Aftershocks were not observed in the case of the Colombian shock.

An obvious extension of the excitation criterion would be to sum vectorially the spectra of many earthquakes recorded at many stations (Mendiguren 1972c). The spectra for each shock should be corrected for their corresponding source mechanism. This is similar to the super-resolution technique proposed by Gilbert (1970) to separate singlets of each multiplet.

Records of different components, namely horizontal and vertical, or records from different types of instruments could also be combined. It should be possible to collect systematically data for many years and continuously improve the resolution of the method and the accuracy of the measured eigenperiods. The use of many earthquakes is specially desirable because, as shown in Section 5, the epicentre location and the arbitrary distribution of stations introduce a bias in the eigenperiod determination which may be larger than the standard deviation of the average.

The excitation criterion can also be applied to other types of geophysical observations where the excitation of the different superimposed signals can be theoretically predicted.

### Acknowledgments

Most of the material presented in this paper is part of the author's Ph.D. Thesis, Massachusetts Institute of Technology, August 1972. I am very grateful to K. Aki

for his continuous and generous advice during this study. I am also indebted to F. Press, D. Davies and M. N. Toksöz for many suggestions and encouragement. I thank the authorities of MIT Lincoln Laboratory, Group 22 for extensive use of their facilities. This study was partially supported by NSF Grant GA-14812 and contract AF49(638)-1763.

Department of Earth and Planetary Sciences  
Massachusetts Institute of Technology  
Cambridge, Massachusetts 02139

### References

- Aki, K., 1967. Scaling law of seismic spectrum, *J. geophys. Res.*, **72**, 1217-1231.
- Aki, K., 1966. Generation and propagation of G waves from the Niigata earthquake of June 16, 1964. Part 1. A statistical analysis, *Bull. earthq. Res. Inst., Tokyo*, **44**, 23-72.
- Alsop, L. E. & Brune, J. N., 1965. Observations of free oscillations excited by a deep earthquake, *J. geophys. Res.*, **70**, 6165-6174.
- Benioff, H., Press, F. & Smith, S., 1961. Excitation of the free oscillations of the earth by earthquakes, *J. geophys. Res.*, **66**, 605-619.
- Blackman, R. B. & Tukey, J. W., 1958. *The measurement of power spectra*, Dover Publications, New York.
- Brune, J. N., 1964. Travel times, body waves, and normal modes of the earth, *Bull. seism. Soc. Am.*, **54**, 2099-2128.
- Derr, J. S., 1969. Free oscillation observations through 1968, *Bull. seism. Soc. Am.*, **59**, 2079-2099.
- Dratler, J., Farrell, W. E., Block, B. & Gilbert, F., 1961. High-Q overtone modes of the Earth, *Geophys. J. R. astr. Soc.*, **23**, 399-410.
- Dziewonski, A. M. & Gilbert, F., 1972a. Observations of normal modes from 84 recordings of the Alaskan Earthquake of 1964 March 28, *Geophys. J. R. astr. Soc.*, **27**, 393-446.
- Dziewonski, A. M. & Gilbert, F., 1972b. *Overtones of spheroidal normal modes in a period range from 100 to 250 seconds*, paper presented at the 9th International Symposium on Geophysical Theory and Computers, The University of Alberta, August 1972.
- Gilbert, J. F., 1970. Progress in the inverse normal mode problem, *E. O. S. Transactions A.G.U.*, **51**, 734.
- Haddon, R. A. W. & Bullen, K., 1969. An earth model incorporating free Earth oscillation data, *Phys. Earth Planet. Int.*, **2**, 35-49.
- Hagiwara, T., 1958. A note on the theory of the electromagnetic seismograph, *Bull. earthq. Res. Inst., Tokyo*, **36**, 134-164.
- Johnson, C., 1972. *Regionalized earth models from linear programming methods*, Master's Thesis, Department of Earth and Planetary Sciences, Massachusetts Institute of Technology.
- Kanamori, H., 1970. Velocity and Q of mantle waves, *Phys. Earth. Planet. Int.*, **4**, 289-300.
- Mendiguren, J., 1972a. *Source mechanism of a deep earthquake from analysis of world wide observations of free oscillations*, Ph.D. Thesis, Massachusetts Institute of Technology, August 14, 1972.
- Mendiguren, J., 1972b. *Identification of free oscillation spectral peaks using the excitation criterion*, paper presented at the 9th International Symposium on Geophysical Theory and Computers, The University of Alberta, August 1972.
- Mendiguren, J., 1972c. Identification of free oscillation spectral peaks using the excitation criterion, *E. O. S. Transactions A. G. U.*, **53**, 1050.

- Mendiguren, J., 1973. High resolution spectroscopy of the Earth's free oscillation, knowing the source mechanism, *Science*, **179**, 179-180.
- Mitchell, B. J. & Landisman, M., 1969. Electromagnetic seismograph constants by least-square inversion, *Bull. seism. Soc. Am.*, **59**, 1335-1348.
- Ness, N. F., Harrison, J. C. & Slichter, L. B., 1961. Observations of the free oscillations of the earth, *J. geophys. Res.*, **66**, 621-629.
- Nowroozi, A. A., 1965. Eigenvibrations of the earth after the Alaskan earthquake, *J. geophys. Res.*, **70**, 5145-5160.
- Nowroozi, A. A., 1972. Characteristic periods of fundamental and overtone oscillations of the earth following a deep-focus earthquake, *Bull. seism. Soc. Am.*, **62**, 247-274.
- Press, F., 1968. Earth models obtained by Monte Carlo inversion, *J. geophys. Res.*, **73**, 5223-5234.
- Press, F., Ben-Menahem, A. & Toksöz, N., 1961. Experimental determination of earthquake fault length and rupture velocity, *J. geophys. Res.*, **75**, 4965-4976.
- Saito, M., 1967. Excitation of free oscillations and surface waves by a point source in a vertically heterogeneous earth, *J. geophys. Res.*, **72**, 3689-3699.
- Smith, S. W., 1966. Free oscillations excited by the Alaskan earthquake, *J. geophys. Res.*, **71**, 1183-1193.
- Toksöz, M. N. & Anderson, D. L., 1963. *Report contract AF-AFOSR-25-63*, California Institute of Technology.
- Wiggins, R. A., 1968. Terrestrial variational tables for the period and attenuation of free oscillations, *Phys. Earth Planet. Int.*, **1**, 201-266.
- Wiggins, R. A., 1972. The general linear inverse problem: Implication of surface waves and free oscillations for earth structure, *Rev. Geophys. Space Phys.*, **10**, 251-285.

## Appendix

### Data processing

Records of the three components long period seismograph at 82 WWSSN stations were digitized. Since, for most of the records, the shortest period present was longer than 8 s, the records were digitized at an interval of 4 s to avoid the aliasing effect. In a few cases, where high frequencies were present, the digitizing interval was reduced to 2 s. The starting time of digitization was taken as early as practically possible, but in most cases, the first train of higher modes could not be included because the record trace was off scale. The digitization of each record was terminated when a clear train of surface waves was no longer visible. The resulting record length ranged from 4 to 18 h. The digitized records were corrected for recording drum drift (Mitchell & Landisman 1969). In order to save computation time when computing the spectra, the number of digitized points was reduced to one fourth by successive averaging over 9, 7, 5 and 3 points (Blackman & Tukey 1958). Then one out of every four points was taken, increasing the time interval between points to 16 s. In addition, the digitized records were high-pass filtered, taking out those periods longer than 700 s.

Since the theoretical spectra are given for the radial, co-latitudinal and azimuthal components, the N-S and E-W records of each station were vectorially summed to synthesize the co-latitudinal and azimuthal components. The resultant records were analysed using the fast Fourier transform over 16384 points. In the next step, the spectra were corrected for instrument response (Hagiwara 1958) and for the low-pass filter response of the decimation procedure.

A digitized version of the Nana strainmeter record, with readings at every 60 s, was provided by Drs S. Smith and D. Anderson. The effect of Earth tides was eliminated through high-pass filtering.

All the theoretical and observed spectra shown in the figures of this study were multiplied by  $\omega^2$  for an adequate graphical representation.

*Comments of the individual peak identifications*

The measured eigenperiods were considered reliable and reported in this study only when the measurement was not affected by interfering modes or noise. Large peak amplitude compared to the amplitude of the surrounding noise and a smooth and symmetrical peak shape were considered indications of small interference. In addition, the magnitude of the standard deviation and the stability of the measurements among different subsets were taken into account to judge the reliability of each measured eigenperiod. An additional critical test before reporting an identification was to plot the measured eigenfrequencies as a function of  $n$  (co-latitudinal order number, e.g.  ${}_0S_n$ ) and require a close fit to a smooth curve. All these elements were taken into account to accept or reject identifications.

The theoretical eigenfrequency for the HBI-6 Earth model corresponding to each mode being identified is indicated in Figs 14-28 with a larger vertical tick on the frequency axis.

**${}_0S$  modes.** The fundamental spheroidal mode  ${}_0S$  dominates the vertical displacement spectra above 160-s period and the identified peaks have a large amplitude over the surrounding noise.

**${}_1S$  modes.** These modes are heavily interfered with the  ${}_0S$  modes. The reported peaks are those which satisfy most of the tests for a reliable measurement. For example in the case of  ${}_1S_{39}$ , Fig. 17, the identified peak is surrounded by other large amplitude peaks but the identification is reliable because the measured eigenfrequency is exactly the same for each of the four stations subsets, see Table I.

**${}_2S$  modes.** In general these are modes well observed on the co-latitudinal component.

**${}_3S$  modes.** Spectral peaks have been observed from  ${}_3S_5$  at 415 s to  ${}_3S_{58}$  at 87 s.  ${}_3S_9$  is a special case with a large signal to noise ratio (Fig. 33) but a large standard deviation. The reported eigenperiod satisfies the required smoothness in the period  $v. n$  plot. Observed on the co-latitudinal component.

**${}_4S$  modes.** Observed within a short frequency range, its peaks are well developed on the co-latitudinal component.

**${}_5S_0$  modes.** These modes are well excited and the identifications are very reliable. Observed on the co-latitudinal component.

**${}_6S_0$  modes.** These modes, like the  ${}_1S$  modes were observed in the vertical component, and they show more interfering noise than those spheroidal modes observed in the co-latitudinal component.

**${}_0T$  modes.** Reliable measurements have been done up to  ${}_0T_{30}$ . For larger  $n$  values the lateral heterogeneities of the Earth affected the spectra to the extent that the laterally homogeneous Earth model is not valid any more (Mendiguren 1972a) and the excitation criterion fails to render accurate results.

**${}_1T$  modes.** Modes up to  ${}_1T_{44}$  have been identified. These modes contain energy at larger depth than the  ${}_0T$  modes and are not so affected by the lateral heterogeneities of the upper 200-300 km (Mendiguren 1972a).

**${}_2T$  and  ${}_3T$  modes.** Only a few isolated groups of modes have been observed with sufficient clarity to be reported.

*WWSSN stations used in this study*

The code names of the stations used in this study are the following: AAE, AAM, ADE, AFI, AKU, ALO, ANP, ARE, ATL, ATU, BEC, BHP, BKS, BOG, BUL, CAR, CHG, COL, COP, COR, CTA, DUG, ESK, FLO, GDH, GIE, GOL, GRM, GUA, HKC, HNR, IST, JCT, JER, KBL, KEV, KIP, KOD, KON, KTG, LAH, LEM, LON, LPA, LPB, MAL, MAT, MSH, NAT, NDI, NOR, NUR, OXF, PDA, PMG, POO, PTO, QUE, QUI, RAB, RAR, RIV, SBA, SCP, SDB, SHA, SHI, SHK, SHL, SJG, SNG, STU, TAB, TAU, TOL, TRI, TRN, TUC, UME, VAL, WEL, WES, WIN.

Summary of Publications for the Entire Contract Period

- Andrews, D.J., Numerical simulation of sea-floor spreading, J. Geophys. Res., 77, 6470-6481, 1972.
- Andrews, D.J., A numerical method for creep deformation of solids, J. Comp. Phys., 12, 275-279, 1973.
- Andrews, D.J. and S. Shlien, Propagation of underground explosion waves in the nearly elastic range, Bull. Seism. Soc. Am., 62, 1691-1698, 1972.
- Bakun, W.H., Focal depths of the 1966 Parkfield, California earthquake, J. Geophys. Res., 77, 3816-3822, 1972.
- Boore, D.M., K. Aki, and T. Todd, A two-dimensional moving dislocation model for a strike-slip fault, Bull. Seism. Soc. Am., 61, 177-194, 1971.
- Boore, D.M., K. Iarner, and K. Aki, Comparison of two independent methods for the solution of wave scattering problems: response of a sedimentary basin to vertically incident SH waves, J. Geophys. Res., 76, 558-569, 1971.
- Derr, J.S., Discrimination of earthquakes and explosions by the Rayleigh wave spectral ratio, Bull. Seism. Soc. Am., 60, 1653-1668, 1970.
- Helmberger, D.V. and G.B. Morris, A travel time and

- amplitude interpretation of a marine refraction profile:  
primary waves, J. Geophys. Res., 74, 483-494, 1969.
- Helmberger, D.V. and G.B. Morris, A travel time and  
amplitude interpretation of a marine refraction profile:  
transformed shear waves, Bull. Seism. Soc. Am., 60,  
593-600, 1970.
- Helmberger, D.V. and R.A. Wiggins, Upper mantle structure  
of midwestern United States, J. Geophys. Res., 76, 3229-  
3245, 1971.
- Hirasawa, T. and M.J. Berry, Reflected and head waves from a  
linear transition layer in a fluid medium, Bull. Seism.  
Soc. Am., 61, 1-26, 1971.
- Hirasawa, T., Radiation patterns of S waves from underground  
nuclear explosions, J. Geophys. Res., 76, 6440-6454, 1971.
- Husebye, E.S., Direct measurement of  $dT/d\Delta$ , Bull. Seism. Soc.  
Am., 59, 717-727, 1969.
- Husebye, E. and R. Madariaga, The origin of precursors to core  
waves, Bull. Seism. Soc. Am., 60, 939-952, 1970.
- Julian, B.R., Regional variations in upper mantle structure in  
North America (abstract), EOS Trans. Am. Geophys. Un.,  
51, 359, 1970.
- Mack, H., Twenty- to eighty-second period characteristics of

nuclear explosions recorded at LASA, in Copies of Papers Presented at Woods Hole Conference on Seismic Discrimination, 1 (ARPA), July 20-23, 1970.

Mack, H., Multipathing of Rayleigh waves generated by Milrow, in Copies of Papers Presented at Woods Hole Conference on Seismic Discrimination, 2 (ARPA), July 20-23, 1970.

Mendiguren, J.A., Identification of free oscillation spectral peaks for 1970 July 31, Columbian deep shock using the excitation criterion, Geophys. J. Roy. Astr. Soc., 33, 281-321, 1973.

Minear, J.W. and M.N. Toksöz, Thermal regime of a downgoing slab and new global tectonics, J. Geophys. Res., 75, 1397-1419, 1970.

Saito, M., Excitation of free oscillations and surface waves by a point source in a vertically heterogeneous earth, J. Geophys. Res., 72, 3689-3699, 1967.

Saito, M., Synthesis of rotational and dilatational seismograms, J. Phys. Earth, 16, 53-61, 1968.

Shlien, S. and M.N. Toksöz, Automatic event detection and location capabilities of large aperture seismic arrays, Bull. Seism. Soc. Am., 63, 1275-1288, 1973.

Shlien, S. and M.N. Toksöz, Automatic phase identification with

with one and two large aperture seismic arrays, Bull. Seism. Soc. Am., in press, 1973.

Sleep, N., Teleseismic P-wave transmission through slabs, Bull. Seism. Soc. Am., 63, 1349-1373, 1973.

Sleep, N. and M.N. Toksöz, Evolution of marginal basins, Nature, 233, 548-550, 1971.

Toksöz, M.N., J.W. Minear, and B.R. Julian, Temperature field and geophysical effects of a downgoing slab, J. Geophys. Res., 76, 1113-1138, 1971.